DOT/FAA/AR-00/42

Office of Aviation Research
Washington, D.C. 20591

Thermal Decomposition Mechanism of 2,2-Bis-(4-Hydroxyphenyl)-1,1-Dichloroethylene-Based Polymers

February 2001

Final Report

U.S. Department of Transportation
Federal Aviation Administration

NOTICE

This report is available at the Federal Aviation Administration William J. Hughes Technical Center's Full-Text Technical Reports page: actlibrary.tc.faa.gov in Adobe Acrobat portable document form (PDF).

Technical Report Documentation Page

1. Report No.	2. Government Accession No.	3. Recipient's Catalog No.
DOT/FAA/AR-00/42		

4. Title and Subtitle	5. Report Date
THERMAL DECOMPOSITION MECHANISM OF 2,2-BIS-(4-HYDROXY- PHENYL)-1,1-DICHLOROETHYLENE-BASED POLYMERS	February 2001
	6. Performing Organization Code

7. Author(s)	8. Performing Organization Report No.
Michael L. Ramirez	

9. Performing Organization Name and Address	10. Work Unit No. (TRAIS)
Federal Aviation Administration William J. Hughes Technical Center Airport and Aircraft Safety Research and Development Division Fire Safety Section, AAR-422 Atlantic City International Airport, NJ 08405	11. Contract or Grant No.

12. Sponsoring Agency Name and Address	13. Type of Report and Period Covered
U.S. Department of Transportation Federal Aviation Administration Office of Aviation Research Washington, DC 20591	Final Report
	14. Sponsoring Agency Code AIR-100

15. Supplementary Notes

The FAA William J. Hughes Technical Center Technical Monitor is Richard Lyon. This work was conducted in partial fulfillment of the degree requirements for a masters of science in chemistry, which was awarded to the author by the University of Puerto Rico (Mayaguez) in January 2000.

16. Abstract

This work has been conducted as part of the Federal Aviation Administration's (FAA) efforts to develop fire-resistant materials for commercial aircraft cabins. Polymers based on 2,2-bis-(4-hydroxyphenyl)-1,1-dichloroethylene (bisphenol C, BPC) have thermal and physical properties of bisphenol-A polymers but have an order of magnitude lower heat release in flaming combustion. This is due to a thermal degradation mechanism that yields only char and noncombustible gases in a fire. Two thermoplastics and one thermoset BPC-based polymer were studied to establish the decomposition mechanism of these materials. Thermal gravimetric analysis, differential scanning calorimetry, infrared spectroscopy, chromatography, and mass spectrometry were used separately and in combination to characterize the thermal degradation mechanism. Results showed that the major volatiles are hydrogen chloride (HCl) and the degradation products of the linking group. The rearrangement through stilbenes and acetylenes is responsible for the high char yield when burned.

17. Key Words	18. Distribution Statement
Fire resistance, Polymer, Cabin materials, Thermal decomposition, Bisphenol dichloroethylene chemistry	This document is available to the public through the National Technical Information Service (NTIS), Springfield, Virginia 22161.

19. Security Classif. (of this report)	20. Security Classif. (of this page)	21. No. of Pages	22. Price
Unclassified	Unclassified	70	

TABLE OF CONTENTS

LIST OF FIGURES

LIST OF TABLES

EXECUTIVE SUMMARY

This work has been conducted as part of the Federal Aviation Administration (FAA) efforts to develop fire-resistant materials for commercial aircraft cabins. Polymers based on 2,2-bis-(4-hydroxyphenyl)-1,1-dichloroethylene (bisphenol C, BPC) have thermal and physical properties of bisphenol-A polymers but have an order of magnitude of lower heat release in flaming combustion. This is due to a thermal degradation mechanism that yields only char and noncombustible gases in a fire. Two thermoplastics and one thermoset BPC-based polymer were studied to establish the decomposition mechanism of these materials. Thermal gravimetric analysis, differential scanning calorimetry, infrared spectroscopy, chromatography, and mass spectrometry were used separately and in combination to characterize the thermal degradation mechanism. Results showed that the major volatiles are HCl and the degradation products of the linking group. The rearrangement through stilbenes and acetylenes is responsible for the high char yield when burned.

INTRODUCTION

It has been estimated that as many as 20 percent of the 1153 fatalities on U.S. transport airlines between 1981-1990 were caused by fire. If the aircraft fatal accident rate remains constant, the total number of fire deaths will grow at an annual rate of 4 percent corresponding to the expected increase in commercial air passenger traffic. This is an unacceptable prospect, and the Federal Aviation Administration (FAA) has taken a bilateral approach to reduce the aircraft fatal accident rate. The first approach is to prevent new factors from increasing the accident rate. The second approach is to reduce the number of accidents of the type that have been occurring and to increase the survivability of such accidents through programs in airplane crashworthiness, fire safety, and fire research.

Aircraft cabin fires fall into three general categories: (1) ramp, (2) in-flight, and (3) postcrash. Ramp fires occur when an aircraft is parked at the ramp during servicing. To date, ramp fires have resulted in the loss of property but not the loss of life. However, considering the current cost of a commercial aircraft ($\approx$ \$100 million), ramp fires are a rare but expensive problem.

In-flight fires most often occur in accessible areas such as the galley and are detected and extinguished promptly. In-flight fire incidents are typically caused by electrical failures, overheated equipment, or improper cargo. Recent examples of catastrophic in-flight fires and explosions which claimed the lives of all passengers and crew are the May 1996 ValueJet flight 592 fire which originated in the cargo compartment (110 fatalities), the July 1996 TWA flight 800 fuel tank explosion (230 fatalities), and the September 1998 Swissair Flight 111 which originated above the cockpit ceiling (229 fatalities).

Despite these recent incidents of catastrophic in-flight fires, the vast majority of fatalities attributable to fire in the United States have occurred in postcrash fire accidents [1,2]. Fuel fires, which penetrate the passenger cabin, are the primary ignition source in these accidents, and it is estimated that 40 percent of these fire fatalities can be attributed to smoke and toxic combustion products of burning cabin materials and jet fuel. Newer regulations require a number of fire safety improvements in aircraft cabins including materials flammability upgrades in aircraft manufactured after 1990 which, depending on the accident scenario, may extend the passenger escape time by 2 or more minutes in a postcrash accident involving a fuel fire.

Compartment fires in aircraft, ships, ground vehicles, and buildings are the most severe from a fire safety perspective because enclosed spaces hold heat and combustion products which increase the severity of the fire and its impact on those exposed. Fires in aircraft, space vehicles, ships, and submarines are particularly hazardous because of the small size of the compartments and the difficulty or impossibility of escape. In aircraft, postcrash cabin fires ignited from spilled jet fuel become life-threatening when the cabin materials become involved and the fire propagates through the cabin generating heat, smoke, and toxic decomposition products. Hot combustion products rise from the fire, entraining air and forming a hot, smoky layer just below the ceiling, which deepens as the fire continues to burn. The availability of air influences the products of combustion as well as the intensity of a fire. As oxygen is depleted during combustion, the fraction of carbon monoxide in the smoke increases appreciably and becomes the primary toxicant in a fire. Burning panels fall and ignite seats causing total involvement of the interior. Ignition of accumulated volatiles results in a flashover. FAA full-scale aircraft

cabin measurements of fire hazards (temperature, smoke, oxygen deprivation, carbon dioxide, carbon monoxide, and irritant gases such as hydrogen chloride (HCl) and hydrogen flouride (HF) indicate that these hazards increase markedly at flashover, exceeding individual and combined tolerance limits at that time. Consequently, the time required to reach flashover is a measure of the time available for escape from an aircraft cabin fire.

While commercial aircraft fires involving loss of life are the most publicized, they are in fact, a small fraction ($\approx$ 1%) of fire deaths. In the United States alone about 4000 people die from fire each year with the majority occurring in residences (74%) and motor vehicles (15%). The U.S. Department of Commerce's Bureau of Economic Analysis estimates that the direct value of property loss in the U.S. from fire is $10 billion annually, with other direct and indirect costs (insurance, fire departments, fire protection, medical costs) adding an additional $90 billion per year. Thus, fire consumes about 1%-2% of the Gross National Product (GNP) and is a significant national and international problem.

The burning of a polymeric material can be explained as a cycle [3] (see figure 1) in which external heat causes the polymer to decompose, producing volatile compounds. These gases combust in the presence of oxygen giving off the heat that decomposes the material. This cycle is divided in two processes or zones. The pyrolysis zone in the solid and the gaseous combustion zone. The initial decomposition occurs in the pyrolysis zone in the absence of oxygen in an endothermic process. The solid does not undergo combustion at the surface because of the low diffusion of oxygen at the surface. The chains of the polymers break into smaller pieces. The mechanism for the breaking of these chains may include depolymerization into monomers, random scission into small fragments, or scission of the side chain fragments. When these fragments are small enough, they leave the surface of the material and mix and react with oxygen to form combustion products and heat.

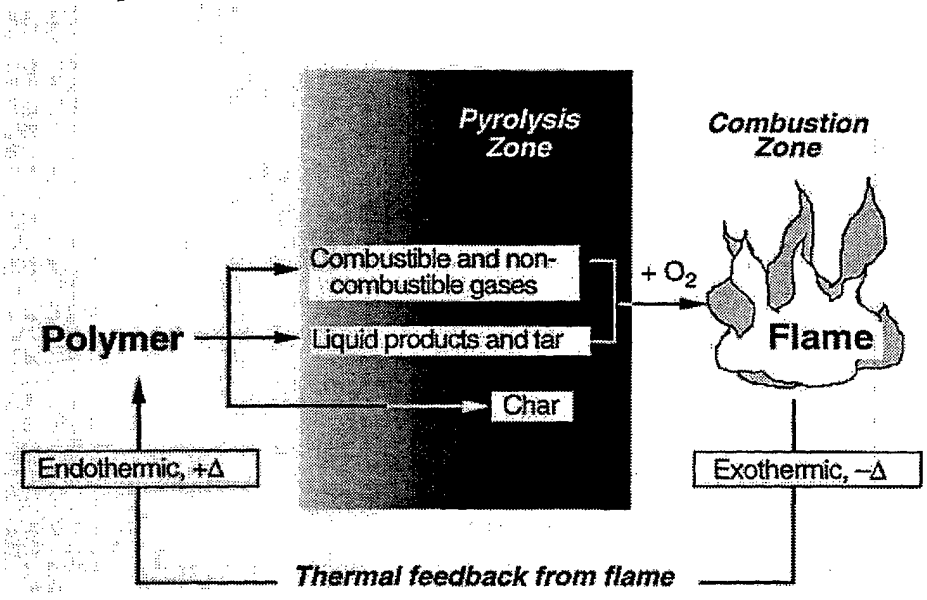

FIGURE 1. MODEL OF THE THERMAL DECOMPOSITION OF POLYMERIC MATERIALS

Organic polymers exhibit a wide range of fire performance from highly flammable to noncombustible. Within this range of fire performance are categories such as flame resistant and fire resistant, which are loosely defined by the results of standardized tests. Flame-resistant materials are typically commodity plastics and resins tested in a vertical orientation as small (1/8- or 1/16-inch-thick) samples which resist burning after ignition by a small (Bunsen burner) flame (e.g., UL 94-V0) or self-extinguish in a specified period of time after removal of the flame (e.g., UL 94 V-1, V-2). Halogen-containing polymers or the addition of fire-retardant chemicals to hydrocarbon polymers is usually sufficient to impart this low level of fire safety. The presence of halogens (chlorine, fluorine, bromine) in the volatile decomposition products interrupts the oxidation process in the flame and reduces the effective heat of combustion (h_c), so that less heat is produced. Flame-retardant chemicals can also promote char formation, which limits the amount of volatile fuel that can be produced by thermal degradation, and insulates the underlying polymer from the flame. If the inert residue or char fraction is μ, the volatile fuel fraction during burning is $1-\mu$. Flame-resistant materials will resist ignition from electrical heating, cigarettes, or small flames but tend to burn readily in a heated (fire) environment, contributing significantly to the spread of fire.

Fire-resistant materials exhibit a higher level of fire performance by not only resisting ignition from small heat sources but also by burning slowly in fire environments to increase human survival time. Fire resistance is determined by the rate of thermal energy (heat) released in flaming combustion for a particular fire environment (radiant heat flux) as measured in a fire calorimeter. Over the past decade, fire science and engineering has advanced considerably and the relationship between the energy/heat release rate of a material and its hazard in a fire is now well established. In fact, heat release rate in flaming combustion is now an FAA regulation for commercial aircraft interior materials and may soon be adopted by other modes of public transportation. The ability to resist ignition or burn slowly when subjected to the radiant energy from a well developed fire (incident heat flux 35-75 kW/m^2) has been achieved by char-forming polymers with high thermal decomposition temperatures, T_p. This high level of fire resistance has been achieved by incorporating thermally stable, conjugated cyclic, or heterocyclic structures into the polymer backbone to minimize the amount of hydrogen which can be abstracted during chain scission to terminate volatile fuel fragments. An unfortunate consequence of high thermal stability is the rigidity of the polycyclic chain, which imparts a dark color to the product and makes high temperature processing necessary for flow (thermoplastic) or cure (thermoset). Polycyclic backbone polymers typically exhibit brittle mechanical behavior and are relatively expensive, limiting the commercial applications for thermally stable fire-resistant materials.

The burning rate of a material is proportional to its heat release capacity, which is related to its chemical structure through the effective heat of combustion of the volatile decomposition products h_C, thermal decomposition temperature T_p, activation energy for pyrolysis E_a, and char yield μ according to reference 4.

$$\frac{\textit{Heat Release}}{\textit{Capacity}} = \frac{h_c(1-\mu)E_a}{eRT_p^2} \qquad (1)$$

Until recently, the fire and material parameters μ, h_c, and T_p could not be varied independently by changing the backbone chemistry of the polymer. Effective heat of combustion is essentially independent of char yield but a change in either of these parameters typically decreases the thermal stability (lowers T_p) so that the overall fire hazard reduction is incremental. Table 1 shows a list of polymers tested at the FAA for heat release rate using a pyrolysis combustion flow calorimeter developed for milligram samples. Included in the list are polymers based on bisphenol-C (BPC) which are seen to be among the lowest values tested. In comparison with polyethylene, these polymers have a heat release capacity which is two orders of magnitude lower.

TABLE 1. HEAT RELEASE CAPACITY VALUES REPORTED FOR MATERIALS TESTED AT THE FAA

Material (abbreviated name), [CAS Registry Number]	Trade Name, Manufacturer/ Supplier	HR Capacity J/g-K	Total HR kJ/g	Char %
Polyethylene (PE) [9002-88-4]	LDPE, Polysciences, Inc.	1676	41.6	0
Polypropylene (PP) [25085-53-4]	Polysciences, Inc.	1571	41.4	0
Polystyrene (PS) [9003-53-6]	Polysciences, Inc.	927	38.8	0
Poly(acrylonitrilebutadiene-styrene) (ABS) [9003-56-9]	ABS Polysciences, Inc.	669	36.6	0
Bisphenol-A Epoxy, catalytic cure (Phenoxy-A) [001675-54-3]	DER-332, Dow Chemical	657	26.0	3.9
Polyhexamethyleneadiapamide [32131-17-2]	Nylon 6/6 Polysciences, Inc.	615	27.4	0
Poly(methylmethacralate) (PMMA) [9011-14-7]	Aldrich Chemical Company, Inc.	514	24.3	0
Dicyclopentadienyl bisphenol	XU-71787, Dow Chemical	493	20.1	27.1
Polycaprolactam	Nylon 6	487	28.7	0
Poly(2,6-dimethyl-1,4-phenyleneoxide) (PPO) [25134-01-4]	Noryl 0.4 IV virgin General Electric	409	20	25.5
Polycarbonate of bisphenol-A (PC) [24936-68-3]	Polysciences Inc., 32-36K MW	359	16.3	21.7
Polyethylenenaphthylate (PEN)	Eastman Chemical Company	309	16.8	18.2
Poly(p-phenylene terephthalamide)	KEVLAR, Dupont	302	14.8	36.1

TABLE 1. HEAT RELEASE CAPACITY VALUES REPORTED FOR MATERIALS TESTED AT THE FAA (Continued)

Material (abbreviated name), [CAS Registry Number]	Trade Name, Manufacturer/ Supplier	HR Capacity J/g-K	Total HR kJ/g	Char %
Bisphenol-A Cyanate Ester [1156-51-0]	AroCy B-10, Ciba Specialty Chemicals	283	17.6	36.3
Tetramethylbisphenol F Cyanate Ester [101657-77-6]	AroCy M-10, Ciba Specialty Chemical	280	17.4	35.4
Epoxy Novolac, catalytic cure (phenoxy-N) [028064-14-4]	DEN-438, Dow Chemical	246	18.9	15.9
Bisphenol-M Cyanate Ester [127667-44-1]	AroCy XU-366, Ciba Specialty Chemicals	239	22.5	26.4
Polyvinylalcohol (99%) (PVOH) [9002-89-5]	Aldrich Chemical Company, Inc.	175	21.3	0
Poly(1,4-phenylenesulfide) (PPS) [9016-75-5]	Aldrich Chemical Company, Inc	165	17.1	41.6
Poly(etheretherketone) (PEEK) [29658-26-2]	450F, Victrex USA	155	12.4	46.5
Novolac Cyanate Ester [P88-1591]	Primaset PT-30, Allied Signal, Inc.	122	9.9	51.9
Polyetherimide (PEI) [61128-46-9]	ULTEM 1000, General Electric	121	11.8	49.2
Poly(etherketoneketone) (PEKK)	G040 (virgin flake), Dupont	96	8.7	60.7
Poly(m-phenylene isophthalamide)	Nomex, Dupont	52	11.7	48.4
Poly(p-phenylenebenzobisoxazole) (PBO) [852-36-8]	PBO, DOW Chemical Co.	42	5.4	69.5
Poly(benzoyl-1,4-phenylene)	POLYX-1000, MAXDEM, Inc.	41	10.9	65.2
Hexafluorobisphenol-A Cyanate Ester [32728-27-1]	AroCy F-10, Ciba Specialty Chemicals	32	2.3	55.2
Bisphenol C Polycarbonate	BPCPC General Electric	29	3.0	50.1
Polyimide (PI) [26023-21-2]	Aldrich Chemical Company, Inc.	25	6.6	51.9

TABLE 1. HEAT RELEASE CAPACITY VALUES REPORTED FOR MATERIALS TESTED AT THE FAA (Continued)

Material (abbreviated name), [CAS Registry Number]	Trade Name, Manufacturer/ Supplier	HR Capacity J/g-K	Total HR kJ/g	Char %
Bisphenol C Cyanate Ester	BPCCE Ciba Specialty Chemicals	13	3.2	58.0
Bisphenol C Polyarylate	BPCPA UMass	18	5.7	50.0
Polybenzimidazole (PBI) [25928-81-8]	CELAZOLE PBI, Hoechst Celanese	17	4.5	73.4
LaRC-CP2	NASA Langley	14	3.4	57
LaRC-CP1	NASA Langley	13	2.9	52

Bisphenol-C (BPC)-based polymers are those based on 2,2-bis-(4-hydroxyphenyl)-1,1-dichloroethylene. Phenol reacts with a carbonyl in a reaction of stoichiometry 2:1 (phenol: carbonyl) catalyzed by an acid (see figure 2). The product of this reaction is a bisphenol. When the carbonyl is from formaldehyde, it is called bisphenol-F (BPF); when the carbonyl is from acetone, it is called bisphenol-A (BPA) which is one of the most commercially used compounds for building polymers and as an additive for other polymeric materials.

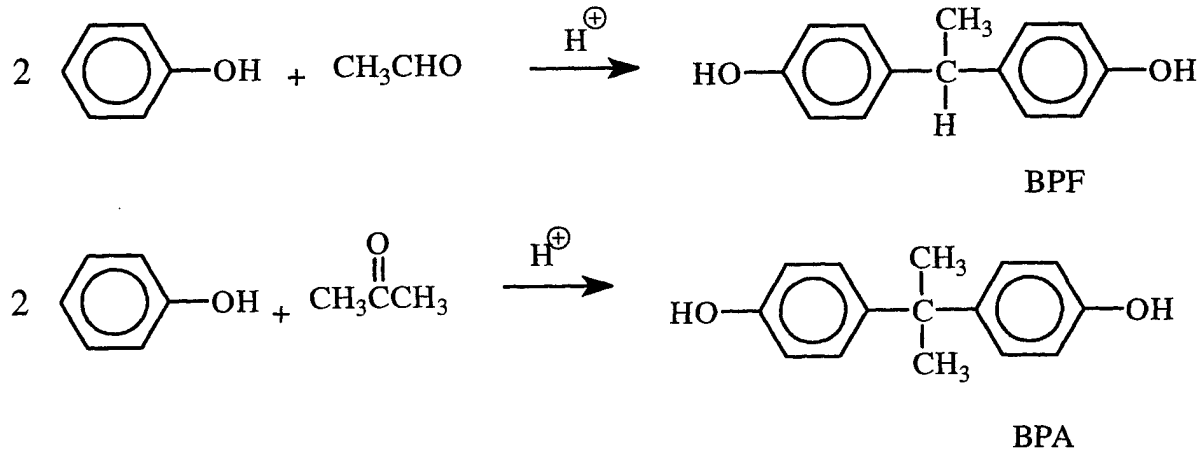

FIGURE 2. SYNTHESIS OF BISPHENOLS

Using this nomenclature, the dehydrochlorinated product of the reaction of chloral and phenol is called bisphenol-C (BPC) (see figure 3).

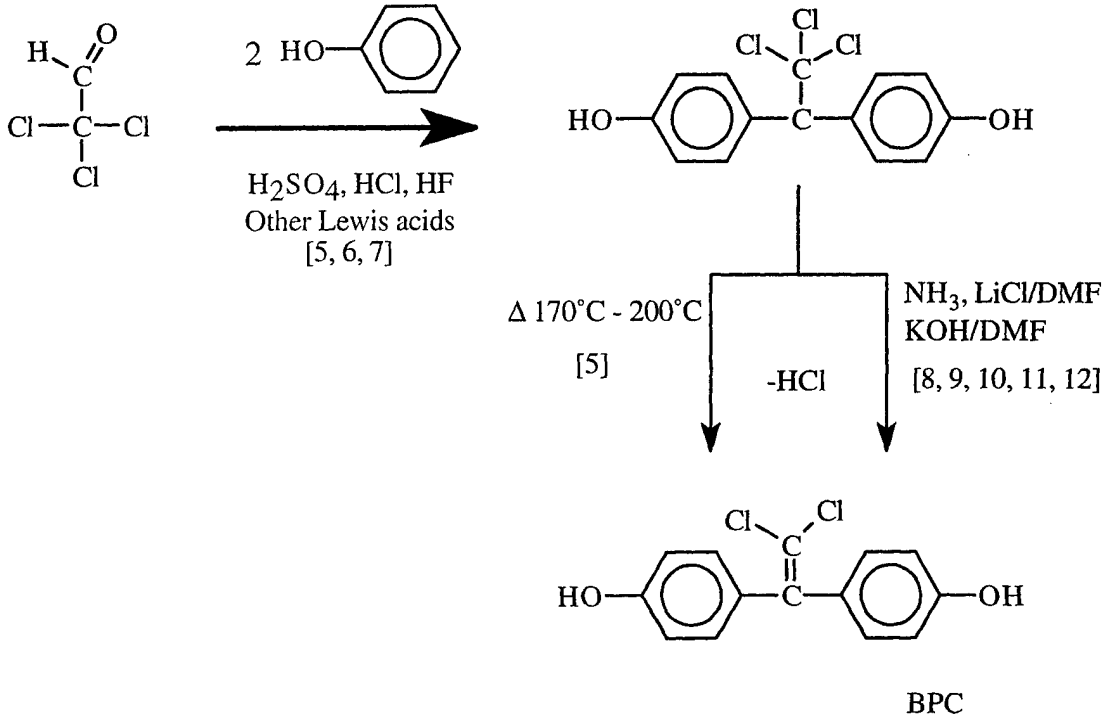

FIGURE 3. SYNTHESIS OF 1,1-DICHLORO-2, 2 BIS (4-HYDROXYPHENYL) ETHYLENE

A comparison of the thermal properties of a BPA polycarbonate and a BPC polycarbonate shows that BPC polycarbonate is more fire resistant because of an increased char yield, high decomposition temperature, and an order of magnitude lower heat release than BPA polycarbonate (see table 2). At the same time, BPC-based materials have equivalent physical and mechanical properties to BPA materials (see table 3), making these materials suitable for fire-resistant transportation applications requiring toughness and durability.

TABLE 2. FIRE-RESISTANT PROPERTIES OF BPA POLYCARBONATE AND BPC POLYCARBONATE

Polymer Repeat Unit	Char Yield (%)	UL-94	Limiting Oxygen Index (% O_2)	Heat Release Capacity (J/g-K)
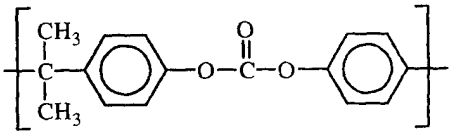	21	V-2	26	359
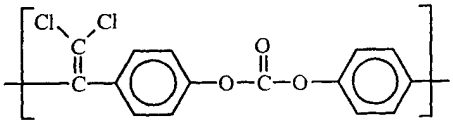	50	V-0	56	29

TABLE 3. PROPERTIES OF POLYARYLATES FROM BPC AND BPA

Properties	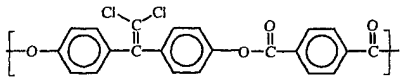	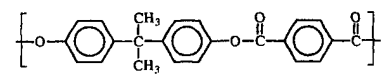
Reduced viscosity of solution in tetrachloroethane	1.2-1.4	1.2-1.4
Thermal degradation temperature (DTGA) (°C)	350-370	320-340
Rupture strength (Kg/cm^2)	750-800	660-720
Volume resistance (ohm*cm)	160	98
Dielectric constant (60 Hz)	20	25
Fire resistance	Nonflammable	flammable
Dielectric loss factor	2.8	6.5

It is the objective of this project to elucidate the mechanism for the unusually high fire resistance of polymers derived from bisphenyl chloroethylene. Studies with model compounds suggest that the thermal decomposition mechanism involves rearrangement of the ethylene chloride bonds to stilbenes and acetylenes [13, 14].

BACKGROUND

Condensation polymers based on chloral and its derivatives are not new. What is new is the discovery of their extremely low energy (heat) release rate in fire environments and the recognition of their potential as enabling materials for cost-effective, fire safe, public transportation. Original publications and patents by Polish and Russian researchers on polymers derived from BPC date back to the 1970s [15] and are summarized in a recent comprehensive review article by Rusanov [5]. There is a comparison in this article of the physical properties as a function of chlorine content of many polycarbonates (see table 4). It demonstrated that as the chlorine content is increased the glass transition temperature (T_g) and ignition resistance increase, while some physical properties decrease. It is concluded that polymers based on 1,1-dichloro, 2,2-diphenyl ethylene posses the best combination of fire resistance and physical properties. In the late 1970s the General Electric Company (GE) patented processes for making polycarbonates from BPC and polyethers directly from bisaryl oxides and chloral [16]. In 1980, GE published a paper describing a flame-resistant polycarbonate based on BPC and reported [17] mechanical, rheological, optical, and thermal properties which were essentially indistinguishable from the BPA analogs which they subsequently commercialized as LEXAN™. The only significant difference between the BPC and BPA polycarbonates reported by General Electric was the lower flammability of the BPC polycarbonates as measured in small flame tests and its lower combustion toxicity when burned.

TABLE 4. PROPERTIES OF CHLORINATED POLYCARBONATES [5]

Structures	Amount of Chlorine (%)	Rupture Strength (MPa)	Glass Transition Temperature (Tg)	Elongation at Break (%)
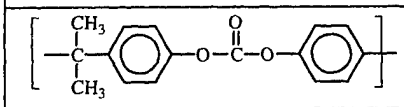	0	149	62	75
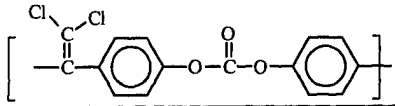	25	168	84	90
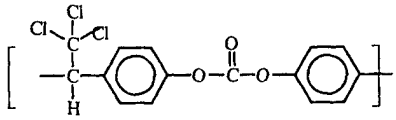	31	220	76	6
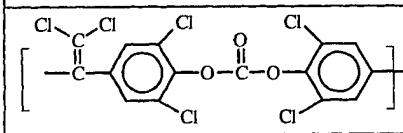	49	250	86	3
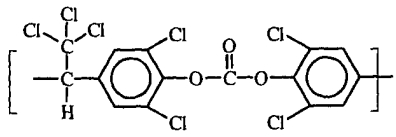	51	273	78	3

There are no published studies on the decomposition mechanism of BPC-based polymers. Brzozowski suggested that the degradation may involve crosslinking through the ethylene bond [5, 15, 18]. In 1976 Suzuki [13] studied the photochemical reaction of 1,1-dibromo, 2,2-diphenylethylene. Irradiation of this compound causes a 1,2-aryl-group migration, resulting in stilbenes and acetylenes (see figure 4).

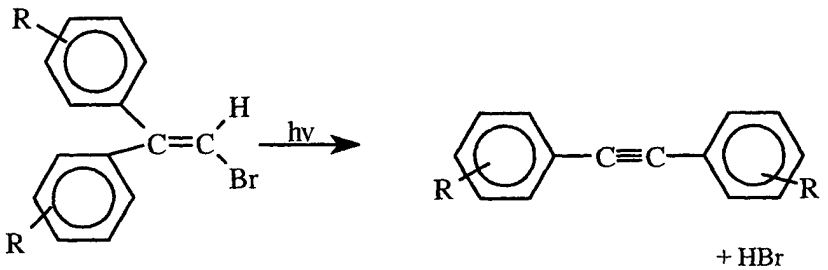

R=
P-OMe
M-Ome
O-Ome
H
P-SMe

50 - 86%

FIGURE 4. PHENYL MIGRATION OF 2,2-DIPHENYL ETHYLENE HALIDES ACCORDING TO SUZUKI [13]

Sket [14] studied the photochemical rearrangement of 1,1-diphenyl-2-halogenated ethylenes finding acetylenes and biphenyl ethylenes (see figure 5). Studies on the reactivity of ethylenes by Quinn [19] showed that introducing alkynes into the linear sequences of aliphatic polycarbonates considerably increases the char yield as well as the limiting oxygen index of the material, but alkynes react exothermally during thermal decomposition. Based in these studies, a mechanism is proposed for the thermal degradation of BPC polymers (see figure 6).

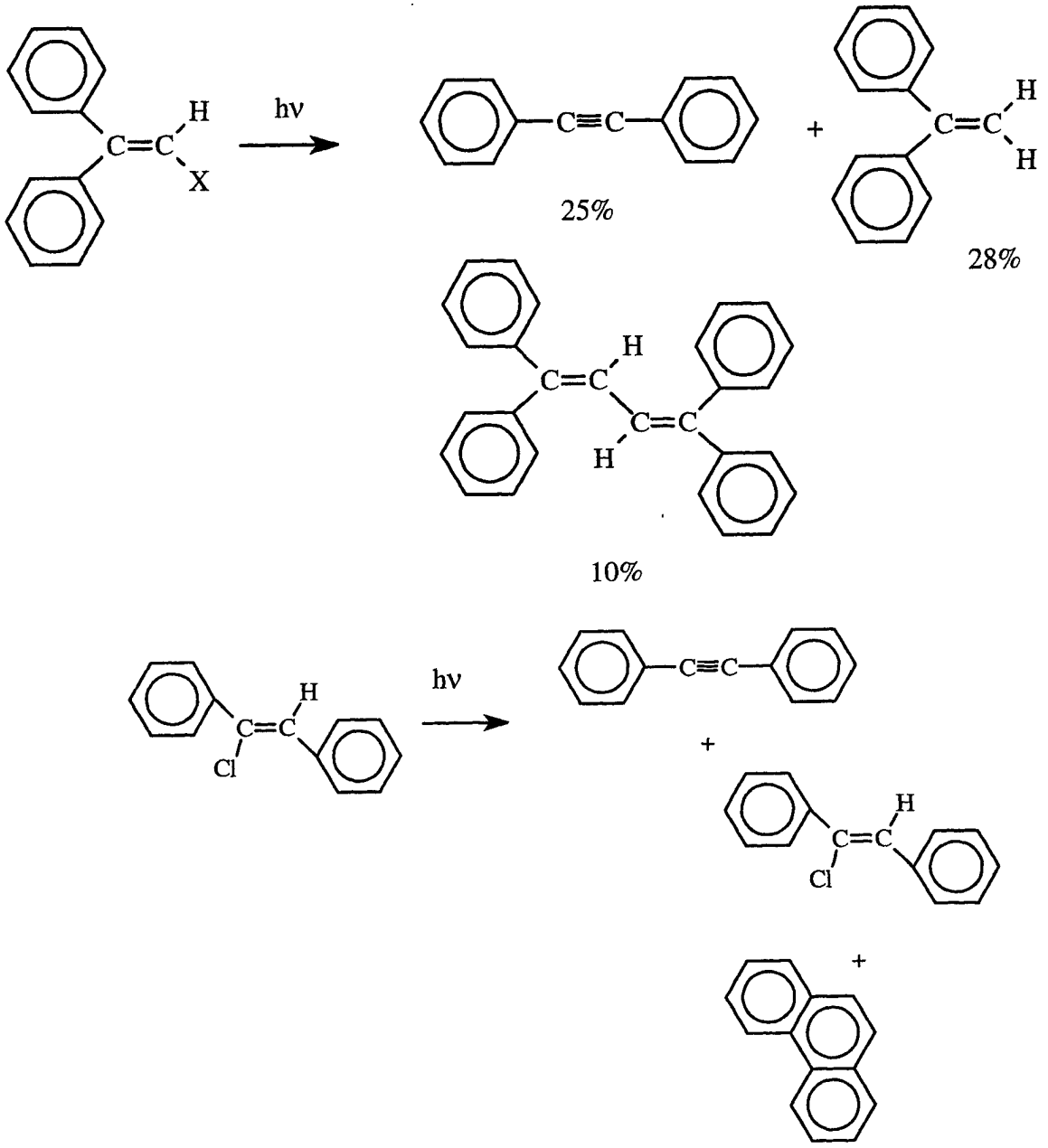

FIGURE 5. REARRANGEMENT OF BIPHENYL ETHYLENE MONOHALIDES INTO ACETYLENES

Infrared (IR) characterization of the thermal degradation of BPA polycarbonate by Politou in 1994 [20] suggested many steps that start by the cleavage of the polymer terminal groups and proceed through rearrangements leading to ethers and esters. The most susceptible group seems to be the carbonate that can be hydrolyzed to carbon dioxide (CO_2). Other works suggest a rearrangement involving the migration of the carbonyl group to an ortho position justifying the crosslinking of polycarbonates and polyester at temperatures between 250° and 300°C [21, 22, 23].

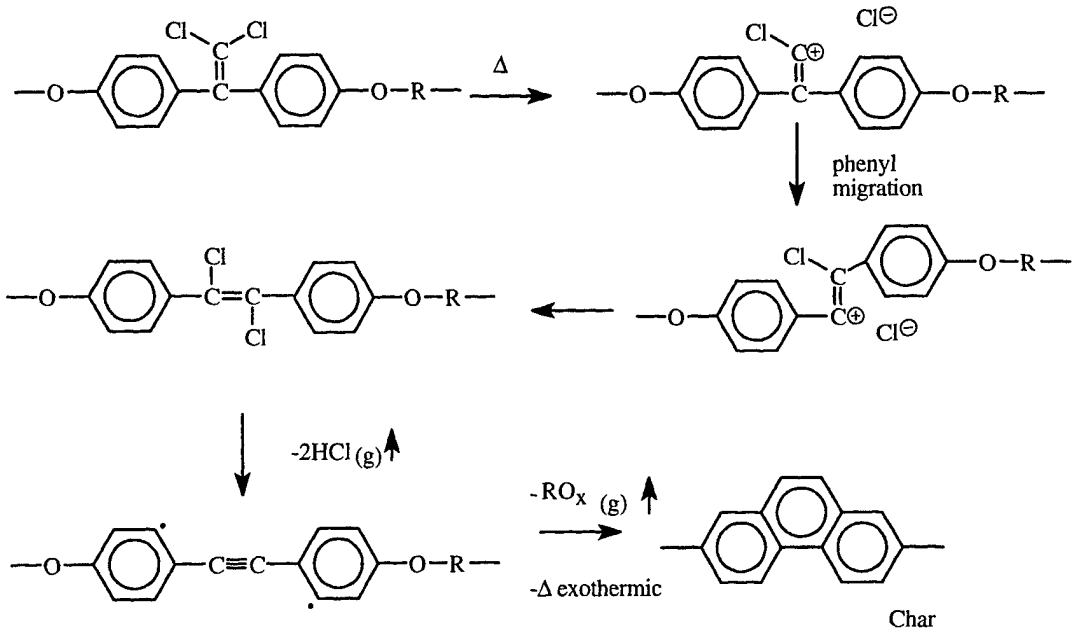

FIGURE 6. PROPOSED MECHANISM FOR THE THERMAL DEGRADATION OF BPC-BASED POLYMERS

EXPERIMENTAL

MATERIALS.

Two aromatic backbone thermoplastic materials, polycarbonate and a polyester (polyarylate) were used in this study. BPA polycarbonate (see figure 7) was provided by GE plastics and the polyarylate (see figure 8) by J. Stewart from the University of Massachusetts [24]. A thermoset polymer consisting of a cyanurate network (see figure 9) was also used for this study. All samples were free of additives or catalysts and were used as received without further purification.

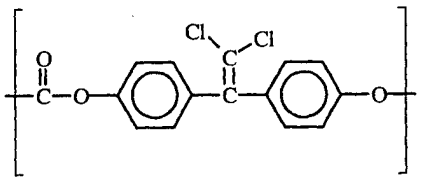

FIGURE 7. BPC-BASED POLYCARBONATE (F.W. = 307 g/mole)

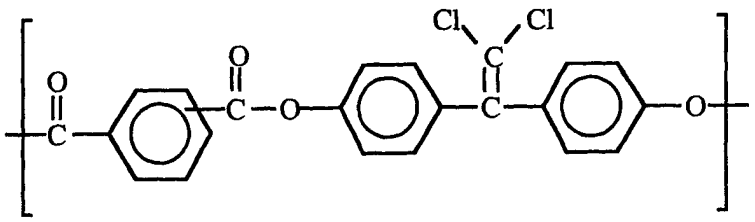

FIGURE 8. BPC-BASED POLYESTER (F.W. = 411 g/mole)

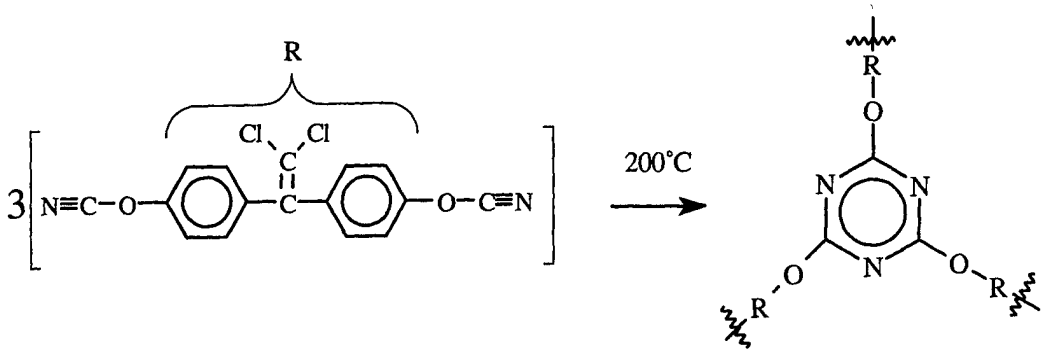

FIGURE 9. BPC CYANATE ESTER (F.W. = 331 g/mole) MONOMER AND CURED NETWORK

Inert environment for thermal analysis and IR spectroscopy was reached using zero grade, ultra-high purity nitrogen (supplied by Matheson). Monomers are soluble in high performance liquid chromatography (HPLC) grade chloroform (supplied by Fisher). Hydrolysis of polycarbonate was carried out using A.C.S. certified NaOH (supplied by Fisher) in HPLC grade methanol (supplied by Fisher).

METHODS.

THERMAL ANALYSIS. The principal thermal analysis techniques used were thermal gravimetric analysis (TGA) and differential scanning calorimetry (DSC). In thermal gravimetric analysis the mass of the sample is recorded as a function of temperature [25]. There are three different modes of TGA; the isothermal TGA, in which the mass of the sample is recorded as a function of time at a certain temperature; the quasistatic TGA, in which the sample is heated to constant mass at each of a series of increasing temperatures; and the dynamic TGA, in which the sample is heated in an environment whose temperature is changing in a predetermined manner (linear rate).

The characteristics for a mass-loss curve for a nonisothermal reaction are illustrated in figure 10. The temperature at which the mass change reaches a magnitude that the thermobalance can detect is the initial temperature (T_i) or incipient decomposition temperature. The temperature at which the cumulative mass change reaches its maximum value corresponding to complete reaction is the T_f. The dotted line is the derivative of the mass-loss curve, with respect to

temperature. In this curve T_p is the temperature for the maximum mass-loss rate. The area under the first derivative curve is the total mass loss for the process.

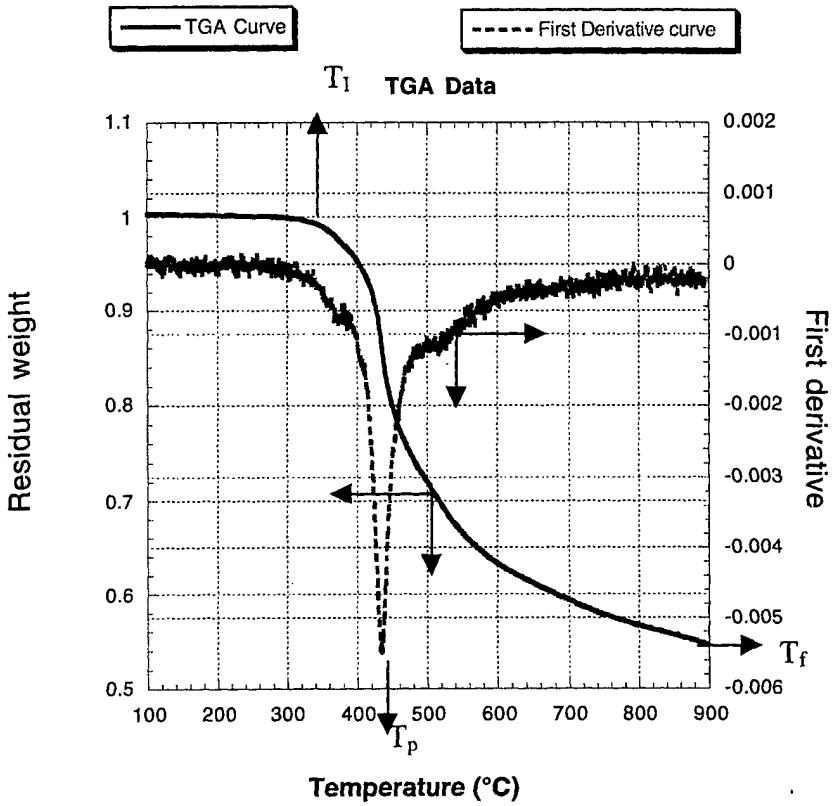

FIGURE 10. THERMAL GRAVIMETRIC ANALYSIS DATA CURVE

A Perkin Elmer Model 7 Thermal Gravimetric Analyzer was used to measure the mass loss of BPC-based polymers. Total mass loss and peak mass-loss rate was calculated. A sample size of about 5 mg was used and a nitrogen flow of 100 cc/min was kept over the sample.

The differential scanning calorimeter (DSC) operates in such a way that energy absorbed or evolved by the sample in the sample cell is counter-balanced by adding or subtracting an equivalent amount of energy to a heater located in the reference cell. This rate of addition or subtraction of energy (power) is what is measured and plotted. Platinum resistance heaters and thermocouples are used in the DSC to monitor the temperature and energy measurements in the design. The continuous and automatic adjustment of heater power necessary to keep the temperature of the reference holder identical to that of the sample holder provides a varying electrical signal equivalent to the thermal energy absorbed or liberated by the sample. This measurement is made directly in differential power units (milliwatts), providing the total energy of the process from the peak areas. Figure 11 shows the heat flow during a chemical process. The downward curve is for an exothermic process. The peak corresponds to the temperature at maximum heat flow for this event. The area of the curve represents the total enthalpy (ΔH) of the thermal transition.

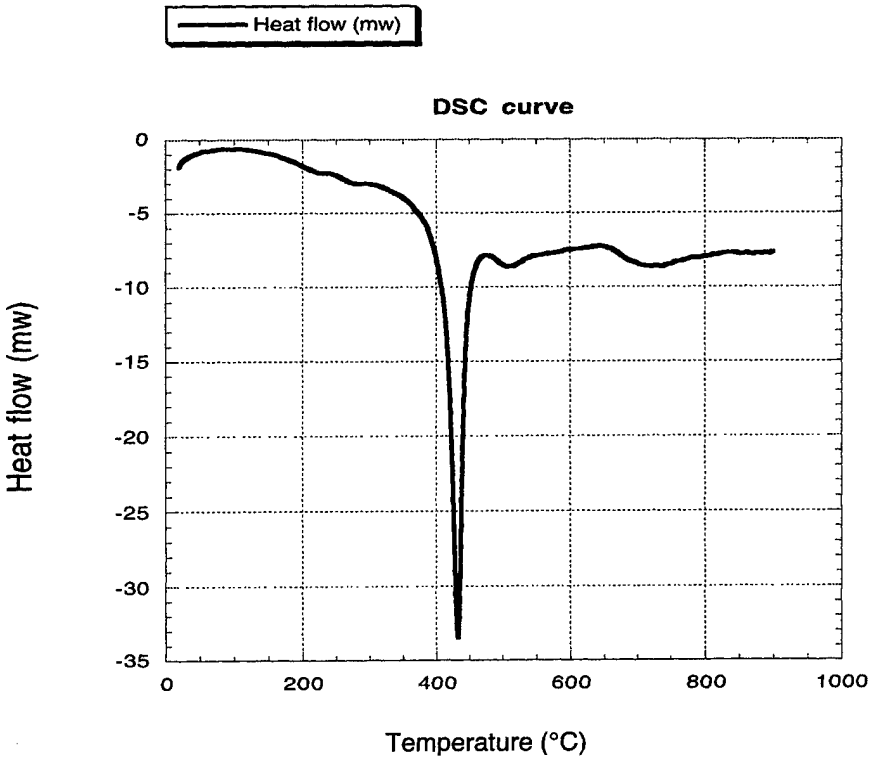

FIGURE 11. DIFFERENTIAL SCANNING CALORIMETRY DATA CURVE

A Differential Scanning Calorimeter (Perkin Elmer Model DSC 7) was used to measure the change in enthalpy (ΔH) of the decomposition process. Samples of 2 to 4 mg were sealed in aluminum DCS pans with holes to allow escape of gaseous decomposition products. Differential scanning calorimetry was run at five or six different heating rates ranging from 5 to 60 K/min with a maximum temperature of 575°C.

Enthalpy was calculated from the heat flow integral. Activation energy (E_a) of the thermal processes was calculated using a method for nonisothermal analysis [26]. To apply this method, the temperature at which a given conversion is reached is determined for several heating rates (β). The fractional conversion, α, is assumed to be equal to the cumulative heat or mass loss at a given temperature, T. The temperature at 50% fractional conversion ($\alpha = 0.5$) was selected for these calculations.

$$\alpha = \frac{H_{(T)}}{H_{total}} \tag{2}$$

The activation energy can be obtained from the heating rate and isoconversion temperature as

$$E_a(\alpha) = R\left[\frac{d\ ln\ \beta}{d(1/T(\alpha)} + 2T(\alpha)\right] \tag{3}$$

where:

$$\frac{d \ln \beta}{d\left(1 / T(\alpha)\right)} \tag{4}$$

is the slope of the plot.

The amount of char produced by a polymer is determined by its structure. Each chemical group in the polymer contributes a characteristic amount to the char residue. Van Krevelen [3, 27] defined the char-forming tendency (CFT) of a chemical group in a polymer as the amount of carbon equivalents in the char per structural unit of polymer or the amount of char per structural unit divided by 12, the atomic weight of carbon. Van Krevelen showed this value to be an additive quantity. Based on the group contribution to the char forming tendency the char residue on pyrolysis can be estimated

$$CR(\%) = \frac{\Sigma N_i CFT_i \times (12\ ^{g}/_{mole})\ x\,100}{\Sigma N_i M_i} \tag{5}$$

Where N_i and M_i are number of moves and the molar mass of structural unit i in the polymer repeat unit. Using the CFT values assigned by Van Krevelen to many groups, the group contribution of the biphenyl chloroethylene unit to the char residue was estimated. A theoretical char yield value was calculated and compared to the TGA data of percentage of residue at 900°C.

ION CHROMATOGRAPHY. Acid gases (HCl) produced during the thermal decomposition of BPC-based polymers were analyzed by ion chromatography.

Ion chromatography is a form of liquid chromatography (LC) that uses ion-exchange resins to separate atomic or molecular ions in solution based on their interaction with the resin stationary-phase. Its greatest utility is for analysis of anions for which there are no other rapid analytical methods [28,29]. It is also commonly used for cations and biochemical species such as amino acids and proteins. Most ion-exchange separations are done with pumps and metal columns. Simple LC columns are used to separate one ion from others in ultra-trace analytical applications.

The column packing for ion chromatography consists of ion-exchange resins bonded to inert polymeric particles (typically 10 μm diameter). For cation separation, the cation-exchange resin is usually a sulfonic or carboxylic acid, (see figure 12) and for anion separation the anion-exchange resin is usually a quaternary ammonium group. For cation exchange with a sulfonic acid group the reaction is

$$\text{-}SO_3\,H^{+}_{(s)} + M^{x+}_{(aq)} \Rightarrow \text{-}SO_3M^{x+}{}_{(s)} + H^{+}{}_{(aq)} \tag{6}$$

where M^{x+} is a cation of charge x, (s) indicates the solid or stationary phase, and (aq) indicates the aqueous or mobile phase.

The partitioning between the stationary and mobile phases depends on the equilibrium constant for this reaction which is

$$K_{eq} = \frac{\left[\text{-}SO_3M^{x+}_{(s)}\right]\left[H^+_{(aq)}\right]}{\left[\text{-}SO_3H^+_{(s)}\right]\left[M^{x+}_{(aq)}\right]} \qquad (7)$$

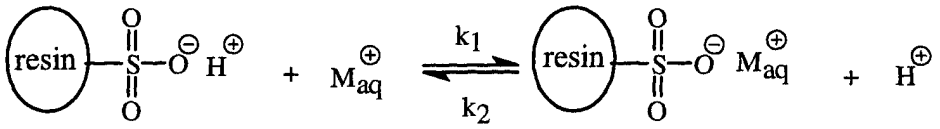

FIGURE 12. CATION EXCHANGE ON THE SURFACE ON THE RESIN

Different cations have different values of K_{eq} and are therefore retained on the column for different lengths of time. The time at which a given cation elutes from the column can be controlled by adjusting the pH ($[H^+]_{aq}$). Most ion-chromatography instruments use two mobile phase reservoirs containing buffers of different pH, and a programmable pump that can change the pH of the mobile phase during the separation.

Ions in solution can be detected by measuring the conductivity of the solution. In ion chromatography, the mobile phase contains ions that create background conductivity, making it difficult to measure the conductivity due only to the analyte ions as they exit the column. This problem can be greatly reduced by selectively removing the mobile phase ions after the analytical column and before the detector. This is done by converting the mobile phase ions to a neutral form or removing them with an eluent suppressor, which consists of an ion-exchange column or membrane. For cation analysis, the mobile phase is often HCl or HNO_3, which can be neutralized by an eluent suppressor that supplies OH^-. The Cl^- or NO_3^- is either retained or removed by the suppressor column or membrane. The same principle holds for anion analysis. The mobile phase is often NaOH or $NaHCO_3$, and the eluent suppressor supplies H^+ to neutralize the anion and retain or remove the Na^+.

Samples of 5-10 mg of the materials were pyrolyzed under a gas flow that carried the gas to the collection column. Nitrogen was used as the carrier gas with a flow of approximately 0.5-0.8 L/min. Pyrolysis was reached using a CDS Pyro 2000 pyroprobe to heat the sample up to 900°C at a constant rate of temperature rise of 10°C/min. The collection column consisted of a tube packed with glass beads, which were covered with NaOH 1.0 M (see figure 13). The gases produced were trapped on this column. The adsorbed gases are then washed out of the column and analyzed by ion chromatography for HCl. A Dionex 500 ion chromatograph with electrical conductivity detector was used for the determination of chloride ions.

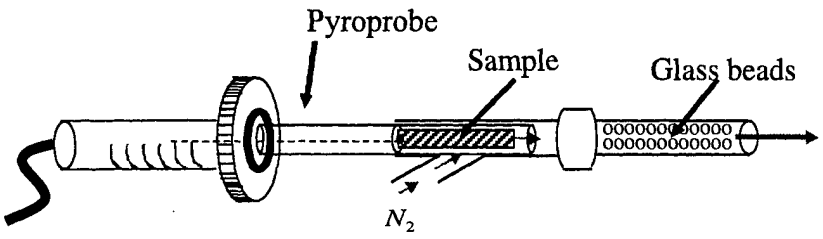

FIGURE 13. DESIGN USED TO COLLECT ACID GASES

INFRARED SPECTROSCOPY. All infrared spectra were taken with a Fourier Transform Infrared (FTIR) spectrometer (Nicolet instruments model Magna 550) with DTGS detector. The spectra were recorded from 4000 to 700 cm^{-1} at a resolution of 4 cm^{-1} using 32 scans.

Gas Analysis by Pyrolysis FTIR. The Brill Cell (CDS Analytical Instruments) is a chamber that permits the analysis of the gases evolved during the thermal decomposition of a material by the combined technique of pyrolysis–FTIR. The Brill Cell is designed to fit into the sample compartment of a standard FTIR bench. It contains IR transparent windows and the filament of the pyroprobe is directly in the light path for immediate acquisition of spectral data (see figure 14). With the filament positioned just below the beam path the sample can be heated rapidly for a single spectrum analysis of the decomposition products of the material or with a constant heating rate for time/temperature studies.

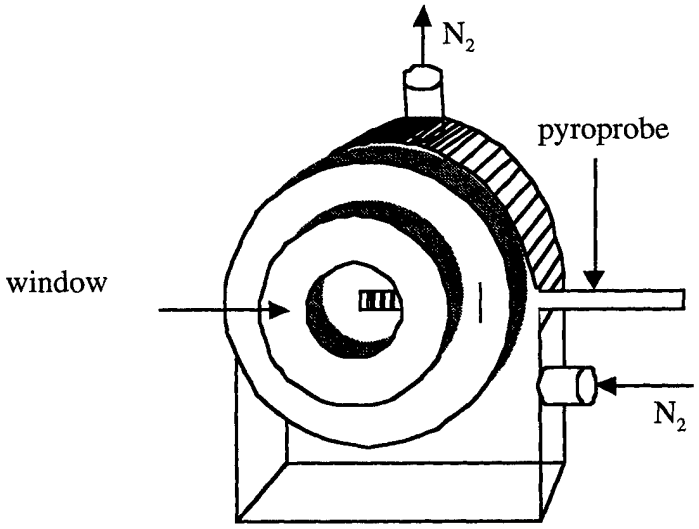

FIGURE 14. BRILL CELL

The Brill Cell can be installed in the FTIR compartment in place of the sample holder. The sample is loaded into the pyroprobe in a quartz tube open at both ends, which permits the sample volatiles to enter the light path. Sample sizes between 100 and 200 µg are recommended for these experiments. The pyroprobe is then placed in the special inlet that allows the filament to be in the optical path. The chamber is then purged with nitrogen to carry out any CO_2 or oxidizer and kept at a temperature sufficient to keep the pyrolysis volatiles in the vapor phase so that they remain in the IR beam (approximately 200° to 300°C). The samples used for this study were pyrolyzed at the same heating rate as was used for TGA studies (10°C/min).

Attenuated Total Reflectance. An Attenuated Total Reflectance accessory (Nicolet instruments model Thunderdome) was used to collect the Infrared spectra of Bisphenol-C-based polymers at room temperature. The attenuated total reflection (ATR) technique is used to obtain the spectra of solids, liquids, and thin films. ATR is performed using an accessory that mounts in the compartment of an FTIR. A schematic diagram is shown in figure 15. The main part of the accessory is a crystal of infrared transparent material of high refractive index. Typical materials used are zinc selenide, KRS-5, and germanium. Mirrors on the accessory bring the infrared radiation to a focus on the face of the crystal. If the light has a proper angle of incidence, it will undergo total internal reflection when passing through the crystal. The infrared energy will reflect off the crystal surface rather than leaving the crystal. In this instance, the crystal acts as a waveguide for the infrared radiation like fiber optic cables. Once the infrared radiation is inside the crystal, a standing evanescent wave is setup. A unique property of the evanescent wave is that it is slightly bigger than the crystal, and so it penetrates a small distance beyond the crystal surface into the sample held in contact with the crystal (see figure 15) [30, 31]. In regions of the infrared spectrum where the sample absorbs energy, the evanescent wave will be attenuated, hence the name attenuated total reflectance. The altered (attenuated) energy from each evanescent wave is passed back to the IR beam, which then exits the opposite end of the crystal and is directed at the detector in the IR spectrometer. The detector records the attenuated IR beam as an interferogram signal, which is inverse Fourier transformed to generate an infrared spectrum. Good contact between the sample and the crystal is critical to ensure the evanescent wave penetrates into the sample. This is why it is imperative that the crystal be kept clean and scratch free and pressure is applied to the sample to achieve good sample/evanescent wave coupling.

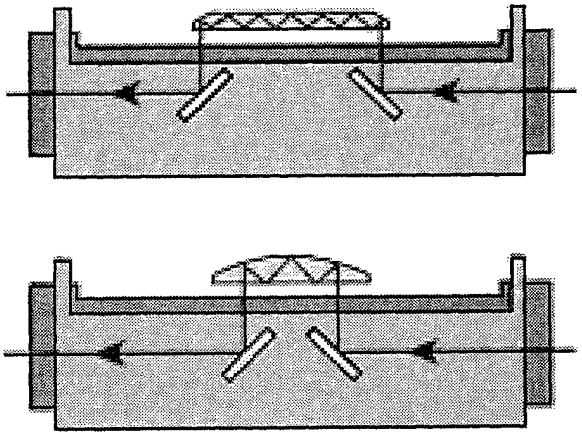

FIGURE 15. DIAGRAM OF THE ATTENUATED TOTAL REFLECTANCE

Infrared Spectroscopy of Solid Films at High Temperatures. A heated cell (CIC Photonics, Inc. Model CIC Hot-One) was used to measure IR absorbance of solid films at high temperature. The cell can be used for studies of thermal degradation of materials as a function of temperature, for studies of phase transitions in polymers, reactions on catalytic substrates, for studies of semiconductor materials, and for other applications on materials research [32]. The standard version is capable of operating at up to 700°C and can control temperature precisely to ±1°C.

The sample holder stands free in an oven-type heater. The sample holder of the Hot-One has a built-in annular stainless steel heater. The heater is held in place by a fitting at the top of the device. An airspace acts as further insulation. The aluminum cell body surrounds the heater. Two Swagelok ports provide for inlet and outlet of coolant. Two additional Swagelok ports have been included for evacuation, pressurization, or flow of gas. A type K thermocouple monitors the sample temperature. The standard configuration has the cell body mounted to the base plate (see figure 16).

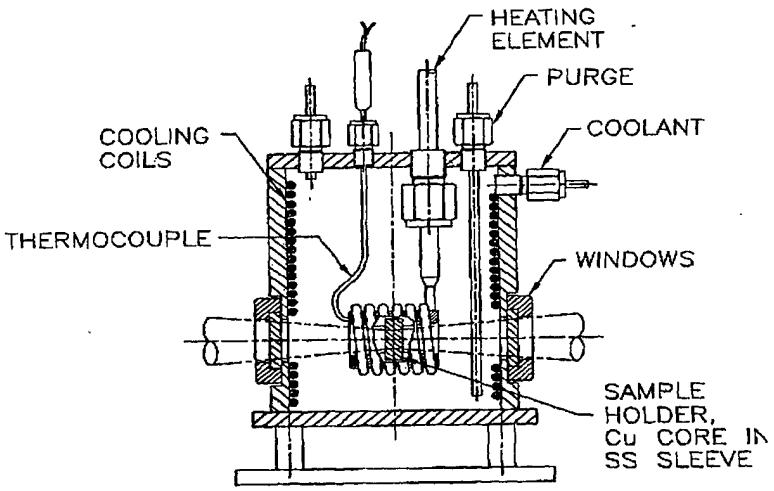

FIGURE 16. DIAGRAM OF THE HEATED CELL USED FOR POLYMER DEGRADATION STUDIES

The sample is loaded into the center of the transmission cell as a free-standing film or on a solid support (e.g., KBr plate) and is surrounded by heating elements, producing uniform heating of its circumference. Power for resistive heating is provided and controlled by an auxiliary microprocessor-based self-timing digital temperature controller.

The transmission cell is either flushed with an inert gas or evacuated during operation. A water-cooling coil wound inside the cell body keeps the cell suitable for using inside the IR and, at the same time, allows for more control of the temperature in a range from room temperature up to 700°C.

Samples of polycarbonate, polyester, and cyanate ester were dissolved in chloroform. A thin film was casted over KBr plates by evaporation of the solvent at 70°C. The sample was then introduced in the heating cell. IR spectra were obtained as a function of temperature from 25° to 675°C. Bands were assigned for most of the functional groups. Reduction of absorbance of bands and appearance of new bands was analyzed to study bond breakage or formation.

Other Studies. When BPC-based polycarbonate is heated to temperatures of about 200°C it turns dark yellow and becomes insoluble. In an effort to understand whether crosslinking occurs and if it is related to the increased fire resistance, some studies were made only on BPC polycarbonate.

Infrared Spectra of the Thermally Degraded Polymer. Samples of approximately 20 mg of BPC PC were heated in a thermogravimetric analyzer (Perkin Elmer model TGA7). The isothermal mass loss history was monitored for each sample. The samples were heated for 30 minutes at 300°, 350° and 400°C. The infrared spectra of the crosslinked material were taken using the ATR accessory in a Magna 550 FTIR spectrometer. A resolution of 4 cm^{-1} was used for all experiments.

Raman Spectra of the BPC-Based Polycarbonate. Samples heated to 300°, 350°, and 400°C for 30 minutes were sent to the University of Massachusetts for Raman spectroscopy. As the samples were highly colored (ranging from yellow to black), the Raman spectra were recorded using long wavelength (1064 nm) excitation in a Fourier transform Raman spectrometer (Bruker model 106, with Nd:Yag laser) to reduce fluorescence. The excitation collection geometry was 180° and spectral resolution was maintained at 4 cm^{-1}. Laser power at the sample was 150 mW. A total of 1024 scans were obtained for each sample.

GAS CHROMATOGRAPHY WITH MASS SPECTROMETER DETECTOR.

Pyrolysis GC-MS. The organic products generated during the thermal decomposition of BPC-based polymers were analyzed by pyrolysis gas chromatography with mass spectrometry detection (Py-GC-MS). In pyrolysis gas chromatography (Py-GC) the fragments generated by pyrolysis are passed through the GC for separation and identification. When using mass spectrometry (MS) detection, the peaks of the resulting chromatogram will contain the mass spectra of the fragments produced by pyrolysis. This data gives direct structural information on the pyrolysis products, providing insight into the bond breaking, rearrangement and decomposition mechanisms of the material [33, 34, and 35]. In many cases, the chromatogram itself serves as a fingerprint of the material and can be used for quality control procedures.

The system used for this study includes a Pyro 2000 pyroprobe (CDS analytical) and an Gas Chromatograph (Hewlett Packard, HP5890, with Electron Impact MS detector). The column was a HP-5 (crosslinked silicone) 25 m x 0.32 mm x 0.52 um film thickness. The interface created by CDS allows isolation of the GC from the pyrolysis unit by an off-line/on-line valve, which permits a purge of air from the pyrolysis unit and interface before connecting to the GC. For reproducibility, it is important to keep a standard method for the GC –MS and for the pyroprobe.

A sample of about 30-100 µg of the material was placed in a quartz tube (1-mm internal diameter x 13 mm length) and the ends sealed with glass wool. The sample is then loaded in the pyroprobe and then placed in the special inlet in the interface. The air in the chamber is purged out. The samples were heated under a helium atmosphere from 200° to 750°C at 10°C/min and held at 750°C for 15 seconds. The pyrolysis products were carried into the capillary column of the GC-MS. The interface and the inlet temperature were kept at 275°C. The initial oven temperature was 40°C for 2 minutes. Then the temperature was increased to 295°C at a heating rate of 10°C/min. The mass range used for the mass spectrometer detector (MSD) was 36 to 400 mass/charge ratio (m/z).

Hydrolysis of the Carbonate Group. Brzozowski [15] has suggested that the thermal degradation of BPC-based polymers starts by crosslinking of the ethylene bond (see figure 17a). Literature indicates that crosslinking of polycarbonates and polyesters is possible through a migration of the paracarbonyl to the ortho position (figure 17b) [21, 22, 23, and 36].

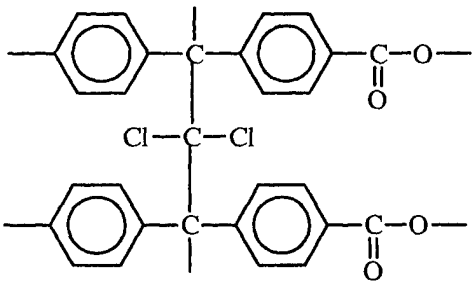

(a) Ethylene Crosslink

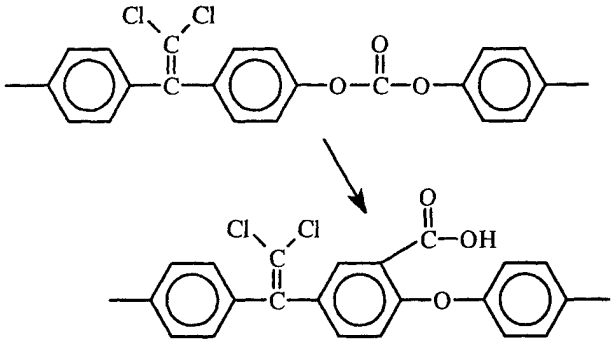

(b) Fries Rearrangement

FIGURE 17. POSSIBLE CROSSLINKING MECHANISMS IN BPC POLYCARBONATE

To investigate the crosslink chemistry, hydrolysis and decarboxylation of the carbonate group was done (see figure 18a) [37, 38, and 39]. If the crosslink is through the ethylene bond, the product will be a high molecular weight partially-crosslinked material (see figure 18b). In contrast, if the crosslink is due to rearrangement of the carbonate group, the product will dissolve in methanol and will show monomer-like structures in a GC-MS analysis (see figure 18c).

Approximately 10 mL of chloroform was added to 20 mg of the crosslinked material. One milliliter of a solution 5% NaOH/methanol was added dropwise with stirring. The mixture was kept stirring for 40 minutes. Then drops of 0.1M HCl were added until the aqueous phase reached pH≈7. The organic part was extracted with methanol and the methanol extract was characterized by GC-MS. A GC model 5890 (Hewlett Packard) with electron capture detector (ECD) and a mass selective detector (model HP 5989B) were used. The column was a HP-5 (crosslinked silicone) 25 m x 0.32 mm x 0.52 um film thickness. After holding the oven at an initial temperature of 40°C for 2 minutes, a heating rate of 10°C/min was used until 295°C. The MSD mass range was 36 to 400 m/z.

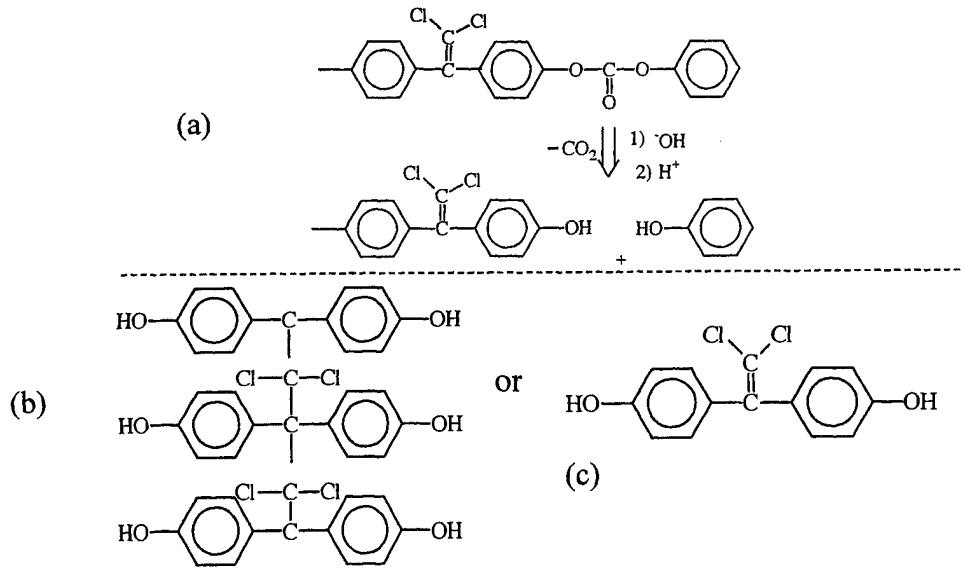

FIGURE 18. HYDROLYSIS OF THE CARBONATE GROUP AND POSSIBLE PRODUCTS

MOPAC Semiempirical Calculations. Computational chemistry was used to estimate the relative ground state energies of possible thermal degradation intermediates and products. Computational molecular models are the result of mathematical equations that estimate the positions and responses of electrons and nuclei. Computer-Aided Chemistry (CaChe) is a software developed by Oxford Molecular that combine molecular modeling with computational models [40].

The mathematical models are divided into classical mechanical and quantum mechanical approaches. Classical mechanics looks at molecules as a collection of atoms and bonds that are treated as balls and springs. Information like atomic radii and spring stiffness are used to find the best positions of atoms.

Quantum mechanical methods solve Schödinger's equation in two ways: semiempirically and ab initio (meaning from the beginning). Semiempirical methods use experimental data to simplify the solution of Schödinger's equation so it can be solved more quickly. Many methods for this simplification have been developed, including Hückle, INDO/S, MNDO, and MOPAC (Molecular Orbital Package).

The CaChe MOPAC application determines both an optimum geometry and the electronic properties of molecules by solving the Schrödinger equation using PM3 semiempirical Hamiltonian developed by J.J. Stewart [41, 42, and 43].

Model compounds representing the different intermediates in the proposed mechanism were drawn in the CaChe Software. The geometry was optimized using the MOPAC semiempirical parameters included in the software. The ground state heats of formation of all the species were calculated to investigate if optimized structural isomers supported or conflicted with the proposed thermal rearrangements.

RESULTS AND DISCUSSION

THERMAL ANALYSIS.

The char yield at 900°C for BPC-based material is about 55% for the polycarbonate and the polyester and 66% for the cyanate ester. This is at least 20% more char yield in each case than the BPA analog (appendix A). When compared to BPA versions of the same material, BPC materials do not have a higher decomposition temperature. In fact, BPC-based polyesters start losing weight at lower temperature than the BPA analog. But the peak of the first derivative curve, which represents the peak mass loss temperature, is approximately the same for all of them (510°C for the polycarbonates and the polyesters and 480°C for the cyanate ester). So increased thermal stability does not account for the higher char yield.

All of the thermal analysis data is summarized in table 5. For BPA polycarbonate the degradation process is athermal ($\Delta H \approx 0$) [44, 22], but the BPC polycarbonate, polyester, and cyanate ester all degrade exothermally. This exotherm was measured and found to be approximately 75 kJ/mole for the polycarbonate and the cyanate ester and 48 kJ/mole for the polyester. This value is very similar to the heat of polymerization of phenyl ethynyl terminal groups used to crosslink imide-based polymers for heat-resistant applications. For this reaction, the change in enthalpy is exothermic at 77-82 kJ/mole of ethynyl group [45] and has a global activation energy, E_a, of 185 kJ/mole. For this report, if the reaction of BPC-based polymers involves ethynyl groups, this value ranged between 144 and 185 kJ/mole.

TABLE 5. THERMAL STUDIES ON BPC POLYMERS

Polymer	M (g/mole)	Heat of Reaction ΔH (J/g)	ΔH (kJ/mole)	Char Yield (%)	E_a (kJ/mole)
Polycarbonate	307.13	-246.2	-75.6	53.1	184.7
Polyester	411.24	-118.1	-48.6	53.3	144.6
Cyanate ester	331.16	-227.5	-75.3	63.2	168.5

Based on the measured residual weights (char yields) of the BPC-based polyester, polycarbonate and cyanate ester at 900°C and tabulated char forming tendencies (CFT) assigned by Van Krevelen [27], it was possible to assign a CFT value of six to the dichloroethylene group attached to para substituted phenyls. Table 6 is a summary of all groups counted for the theoretical char yield and the experimental char yield. Van Krevelen assigned a CFT value of four to a disubstituted benzene [27], meaning that for every disubstituded benzene group there is, on average, a contribution of four carbons to the char.

Based on this value, the CFT contribution of the ethylene chloride bond was estimated to be six. That is, for every two-carbon ethylene chloride bond attached to paraphenylenes, six carbons end up in the char. This is strong evidence that the ethylene bond is incorporating adjacent aromatic carbons into the char. If taken as a group, the bisaryl dichloroethylene group has a CFT value of 14, which is the same value assigned to three fused phenyl rings by Van Krevelen. This suggests that the bisaryl dichloroethylene group degrades by incorporating both phenyls into the carbonaceous char quantitatively. The char yield values were estimated and the measured values are within 5% of the estimated (see table 7).

TABLE 6. CHAR FORMING TENDENCIES VALUES FOR THE GROUPS IN BPC-BASED POLYMERS

Groups	CFT Contribution	Reference
$C{=}CCl_2$	6	This report
	4	[27]
	0	[27]
-O-	-0.1	[27]
-CN	3.7	[27]

TABLE 7. CHAR YIELD VALUES FOR BPC-BASED POLYMERS

Groups	Theoretical Char Yield	Measured Char Yield
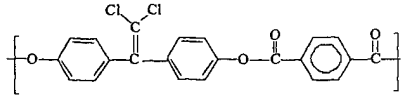	51.9	52.3
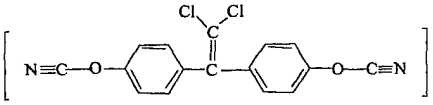	62.9	66.1
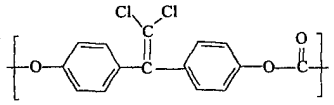	53.1	53.9

INFRARED SPECTROSCOPY OF GASEOUS PRODUCTS.

The infrared spectra of the BPC polymer decomposition products have in common the presence of HCl (appendix B). For the polycarbonate, the main decomposition products are HCl and CO_2. For the polyester, the gaseous products are mainly CO_2 and HCl with very few other organic compounds that were identified by Py-GC-MS. The IR of the cyanate ester decomposition products shows HCl and multiple peaks in the region of 2200 to 2300 cm^{-1} due to isocyanic acid (HOCN) and CO_2. Hydrogen chloride and carbon dioxide are noncombustible gases, which accounts for the low heat release capacity (equation 1); which contains the heat of combustion of the gases as one of the parameters.

DETERMINATION OF GASEOUS HYDROGEN CHLORIDE BY ION CHROMATOGRAPHY.

The amount of HCl produced by the decomposition of BPC-based polymers was measured using ion chromatography, and the results are summarized in table 8. The data represent the percent chlorine content that was collected in the column and measured in the form of chloride anion (Cl^-). The origin of this Cl^- is assumed to be HCl. The rest of the molecular chlorine of the polymers is recovered in the form of halogenated compounds as demonstrated with the GC-MS.

TABLE 8. HYDROGEN CHLORIDE DETERMINATION BY ION CHROMATOGRAPHY

Polymer	M (g/mole)	Weight Percent of Chlorine in Repeat Unit	Percent of Theoretical Cl^- Recovered
Polycarbonate	307	21.7	91.3
Polyester	411	15.5	89.8
Cyanate ester	331	17.7	78.6

PYROLYSIS GC-MS.

The Py-GC-MS data showed that when BPA polymers decompose thermally there is random scission in the chain involving the BPA group and recombination of the gaseous product possibly by radical reactions. This is demonstrated by the diverse methylated and ethylated aromatic products during the pyrolysis of BPA-based polymers (appendix C). The 2,2-bisphenyl-propane unit breaks into phenol, benzene, and other phenyl- or methyl-based volatile compounds. Some products common to all BPA-based materials analyzed are phenol, methyl-phenol, benzene, ethyl-phenol, tetramethyl-phenol, and some monomer. Considering the low char yield of these polymers and the diversity and abundance of the degradation products, reactions involving degradation and breaking of the monomer are favored. The high concentration of organic volatiles will lead to a high heat of combustion for the pyrolysis products and an increase in the heat release rate (equation 1).

For BPC-based materials, reactions involving volatilization of the linking groups between the bisaryl dichloroethylene units are favored. For all BPC-based polymers, CO_2 is the most abundant peak (HOCN for the cyanate ester) so the heat of combustion of the evolved gases from pyrolysis is low.

In the case of the BPC polyester, there are products related to the phthalate linkage such as benzoic acid, biphenyl, benzene, and other products common to the BPA polyester. As expected there are small concentrations of halogenated organic compounds like chlorobenzene, benzoyl chloride, etc.

SEMIEMPIRICAL CALCULATIONS.

Different model compounds related to the proposed mechanism were used in the CaChe software. Table 9 presents the heat of formation for the ethylene bond, the stilbene, the acetylene, and the final carbonaceous structure, presented as phenanthrene. The phenyl migration to the position 1,2 bisphenyl (stilbene) can occur without a big change in formation

energy (ΔH_f= -4 kJ/mole). But the loss of the two chlorines and the formation of the acetylene is an endothermic process requiring 160 kJ/mole. The heat of formation of the final aromatic structure (phenanthrene) indicates that it is more stable than the acetylene (phenanthrene = -156 kJ/mole vs. acetylene = +38 kJ/mole), so if the acetylene is formed, it will rearrange to the more stable aromatic structure (ΔH = -194 kJ/mole) as demonstrated with the heats of formation of these structures. The heats of formation of the products and reactants are consistant with the experimental observations of the reaction as a fast exothermic event.

TABLE 9. CALCULATED HEATS OF FORMATION OF MODEL COMPOUNDS

Structure	Formula	MW (g/mole)	H_f (kJ/mole)
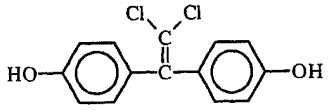 Dichloroethylene Bisphenol	$C_{14}H_{10}O_2Cl_2$	281.13	-148.8
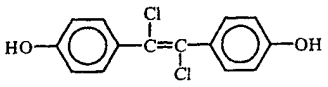 Stilbene Bisphenol	$C_{14}H_{10}O_2Cl_2$	281.13	-141.1
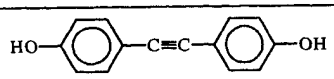 Acetylene Bisphenol	$C_{14}H_{10}O_2$	210.1	38.1
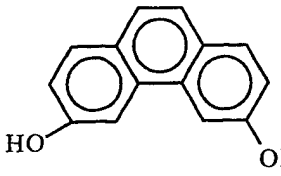 Phenanthrene Bisphenol	$C_{14}H_{10}O_2$	210.1	-156.1

INFRARED SPECTROSCOPY OF SOLID FILMS.

Appendix D contains all of the infrared spectra of the solid film analysis. The bands and the assignments are summarized in tables 10 through 12. Given the fact that most infrared modes of polyatomic systems, especially for compounds as complex as polymers, are likely to have a rather mixed character, the suggested assignments refer only to most predominant character in the mode. All three polymers have in common the strong aryl-O-C ether band in the 1200 cm^{-1} area. This strong band results from the combination of C-O-C stretching and ring vibrations [46] and will give three very strong peaks for the polycarbonate and polyester and two for the cyanate ester [20, 46, and 47].

TABLE 10. BAND ASSIGNMENTS FOR BPC-BASED POLYCARBONATE

Band Position (cm^{-1})	Assignment
3040	Aromatic C-H stretch
1774	C=O stretch of OCOO
1600	Quadrant C-C bond ring stretching
1504	Semicircle ring stretching
1408	Semicircle ring stretch
1227	Asymmetric stretch of Ph-O-C
1189	Asymmetric stretch of Ph-O-C
1161	Asymmetric stretch of Ph-O-C
1017	C-C in plane bend
974	C-Cl of $C=C(Cl_2)$
887	Symmetric OCOO stretch
861	Aromatic C-H OOP deformation
760	C-H wagging/ monosubstituted ring

TABLE 11. BAND ASSIGNMENTS FOR BPC-BASED POLYESTER

Band Position (cm^{-1})	Assignment
3748	Phenol O-H stretch
1736	Ester C=O stretch of O-COPh
1600	Quadrant C-C ring stretch
1502	Semicircle ring stretch
1407	Semicircle ring stretch
1260	Asymmetric stretch of Ph-O-C
1200	Asymmetric stretch of Ph-O-C
1165	Asymmetric stretch of Ph-O-C
1071	Aromatic C-H and ring
1015	C-C in plane bend
973	C-Cl stretch of $C=C(Cl_2)$
866	Aromatic C-H OOP deformation
768	OOP skeletal vibration of OCOPh
721	C-C ring OOP deformation

TABLE 12. BAND ASSIGNMENTS FOR THE CROSSLINKED BPC CYANATE ESTER

Band Position (cm^{-1})	Assignment
1563	Triazine
1502	Semicircle ring stretch
1459	Semicircle ring stretch
1364	Triazine
1207	Asymmetric stretch of Ph-O-C
1169	Asymmetric stretch of Ph-O-C
1083	Aromatic C-H and ring
1017	C-O-C stretching
973	C-Cl stretching of $C=C(Cl_2)$
861	Aromatic C-H OOP deformation
812	Aromatic C-H OOP deformation
640	In-plane ring bend

There is a band at 975 cm^{-1} that is related to the asymmetric stretch of the C-Cl of the disubstituted ethylene bond. In 1972, Wielgosz [18] identified this band as related to the 2,2-diphenyl1,1-dichloro ethylene bond unit and was located at 980 cm^{-1}. In this report, this band was found between 973 cm^{-1} and 975 cm^{-1}. It has been suggested [48] that the antisymmetric mode of the C-Cl stretch in $C{=}CCl_2$ should occur between 1000 cm^{-1} and 800 cm^{-1} and that the symmetric mode should occur at 600 cm^{-1}. Consequently, the band at 975 cm^{-1} was assigned as the antisymmetric stretch of $C{=}CCl_2$, since it is common to all BPC-based polymers as well as the 2,2 -bis (4-hydroxyphenyl)-1,1 dichloro ethylene monomer. Also, all of the BPC polymers materials share most of the bands related to the aromatic rings. To study the decomposition mechanism, the functional group bands were selected for comparison as well as the band at 975 cm^{-1}, which is related to the 2,2- diphenyl1,1-dichloro ethylene bond group. Also, common bands like the 1500 cm^{-1} (ring) and the 1200 cm^{-1} band, related to the ether link, were observed.

The basic difference between the cyanate ester resin and the cured thermoset is the disappearance of the –CN band at 2230 cm^{-1} (appendix D, figure D-1) and the appearance of a band at 1570 cm^{-1} and another at 1360 cm^{-1} (appendix D, figure D-2) corresponding to the quadrant stretch and semicircle stretch of the triazine ring, respectively. Since this report is about the decomposition of BPC-based materials, just the spectra of the cured BPC-based cyanate ester will be considered.

Figure D-5 contains the infrared spectra of BPC-based cyanate ester at 25°, 100°, 200°, 300°, 400°, 450°, 500°, and 550°C. The spectra show no considerable changes for the first 400 degrees. The band at 975 cm^{-1} is decreasing at the same time as others like the 1500 cm^{-1} semicircle stretch and the 1360 cm^{-1} triazine band. At temperatures above 400°C, the band at 1570 cm^{-1} decreases. Over the same temperature interval the band at 2280 cm^{-1} increases reaching a maximum at 475°C. This pattern suggests unzipping of the cyanurate ring band into the monomer –OCN unit. Above this temperature the 2280 cm^{-1} band decreases again, probably because of the elimination of HOCN which was present in the GC-MS data. The most common model for the degradation of the cyanurate ring involves the production of CO, CO_2, hydrogen cyanate (HCN), and amines [49]. In this report, it is observed that the first step is depolymerization to the original monomer. There is no evidence of amines in the MS data of the present report. But there are two peaks for CO_2 (both with low compatibility with the CO_2 mass spectra). The presence of peaks with 43 and 42 m/z may indicate the presence of HOCN rather than CO_2. Other minor products indicate prevalence of the cyanate (CN) unit. During this process, all the bands contained in the aromatic region (1000 to 1600 cm^{-1}) have been decreasing, as well as the peak at 975 cm^{-1}. Also, the baseline in this area is rising until it fuses with the bands into a broad band from 100 cm^{-1} to 1600 cm^{-1}, suggesting the final degradation of the sample into char with aromatic character (optical blackness of the char) [20].

The two principal events during the decomposition of polycarbonates and polyesters are (1) transfer of the carboxyl group to an ortho position, a rearrangement producing a diaryl ether linkage and crosslinking [20, 21, 23, and 36] and (2) decarboxylation. These rearrangements would increase the char yield of the materials. But also, the thermal stability will depend on the rigidity of the structural unit.

For the polycarbonate, this rearrangement would produce an ether link and benzoic acid in the ortho position (see figure 19).

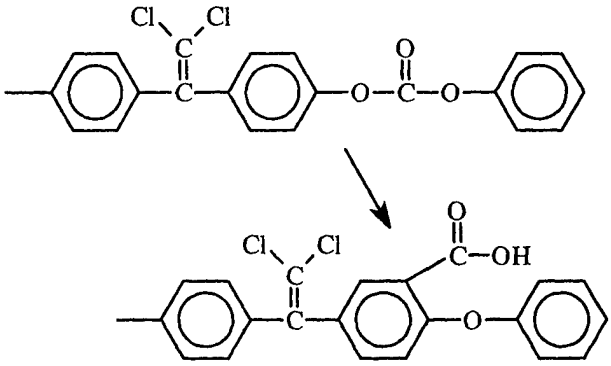

FIGURE 19. POSSIBLE THERMALLY INDUCED REARRANGEMENT FOR POLYCARBONATES

Figure D-6 is a comparison of BPC-based polycarbonate spectra taken during a linear heating program between 30° and 600°C. A band for the diaryl ether should appear at 1240 cm^{-1}, but it is difficult to assign because there is an ether band in the region already. There is no spectroscopic evidence for the benzoic acid. There are no significant bands in the 3000 cm^{-1} to 3500 cm^{-1} region that are related to the oxygen hydrogen (OH) group. The band for the carboxyl (1775 cm^{-1}) group is strong over the entire temperature range. The first band to have a considerable change is the band at 760 cm^{-1}. At 200°C it has lost half the intensity. Since this band is often related to a monosubstituted benzene [20], it has been suggested that this implies the loosening of the terminal ends of the polymer chain or its participation in a rearrangement. The peak at 975 cm^{-1} decreases continuously with increasing temperature until it completely disappears at 475°C. At this point the predominant absorbance bands are the ones in the 1200 cm^{-1} region, the carboxyl peak at 1775cm^{-1}, and the aromatic bands (1600, 1500, 1017 cm^{-1}, etc). At 500°C, the carbonyl band has disappeared, and the remaining bands are of aromatic character which disappear in the broad band characterizing the char by 600°C .

The spectra for the polyester (appendix D, figure D-7) show little evidence for the proposed rearrangement (figure 20).

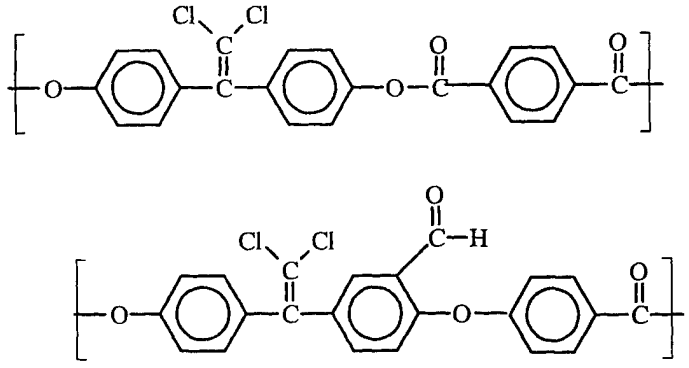

FIGURE 20. PROPOSED REARRANGEMENT OF THE POLYESTER

The expected band for the diaryl ether would appear in the 1240 cm^{-1} region, but this region is dominated by the strong aromatic ether band at 1200 cm^{-1}. But at 150°C, bands at 2800 to 2900 cm^{-1} appear that may correspond to the aldehyde hydrogen [47] that continue increasing to a maximum value at 375°C, after which this band decreases along with all of the other bands. The carbonyl band disappears at 500°C. Above this temperature, only the bands of aromatic character are present until the material becomes opaque to the IR.

It was very difficult to monitor the nature of the degradation of the dychloroethylene using IR spectroscopy because of the small size of the 975 cm^{-1} peak and its proximity to bigger bands so that it was lost in the base line. Also, it is difficult to identify stilbenes and acetylenes in the infrared spectrum because they are symmetric structures. Therefore, it was possible to identify the main steps of the decompositions of the BPC-based polymers, but it was impossible to obtain spectroscopic proof of the proposed mechanism.

The Raman spectra showed no difference between the crosslinked polycarbonate and the material at room temperature (appendix E, figure E-1). The same bands are present until decomposition. At this time most of the bands disappeared. Samples of BPA polycarbonate were exposed to the same heat treatment resulting in the same dark yellow color without any changes in the infrared spectra (appendix E, figure E-2). The polyester has the same behavior when exposed to these temperatures. After 30 minutes at 350°C, the polyester was very dark, but little change was seen in the IR spectra of the crosslinked sample compared to the sample at room temperature. The dark yellow color caused a fluorescence effect that masked the Raman spectra of the sample heated to 400°C. For the other crosslinked samples, there were few differences in the IR spectra caused by heating to 300° and 350°C other than the broadening of the 1000 to 1500 cm^{-1} area. This might be caused by the fluorescence.

The hydrolysis and decarboxylation of the BPC-based polycarbonate at room temperature resulted in BPC monomer-like structure as seen in the fragmentation pattern in the MS spectra (appendix E, figure E-3). When chloroform was added to the crosslinked polycarbonate sample at 300°C, it did not dissolve. Usually chloroform is a good solvent for the BPC-based polymers. But at the first drop of the NaOH solution it dissolved immediately. The GC MS chromatogram of the crosslinked polycarbonate is in appendix E, figure E-4. The chromatogram shows two peaks for the monomer-like fragmentation pattern: one at 23.5 minutes and the other at 22.5 minutes. The chromatogram of the polycarbonate at room temperature has the peak for the monomer at 23.5 minutes, so the peak at 22.5 minutes might be the stilbene rearrangement because they are structural isomers. There is also a peak corresponding to a halogenated acetylene and a main peak, which is a halogenated structure very similar to dicloro diphenyl ethylene (DDE) according to the mass spectral library used for identification (appendix E, figure E-5).

CONCLUSIONS

The fire-resistance efficacy of 1,1,-dichloro-2,2-bis (4-hydroxyphenyl) ethylene-based polymers derives from the unique combination of a high decomposition temperature ($T_p \approx 500°C$), high char yield ($\mu \approx 0.5$), and extremely low effective heat of combustion of the fuel gases ($h_c \approx 3$ kJ/g) during the burning process.

The major products of the decomposition are HCl and volatiles containing the linking groups. The HCl was identified by FTIR and measured using ion chromatography. The pyrolysis GC-MS data show a considerable reduction in the combustible volatile organic compounds compared to BPA versions of the same material. The principal product of the decomposition of BPC-based polyester and BPC-based polycarbonate was CO_2 and for the thermoset resin HOCN and CO_2.

There is no spectroscopic evidence for the stilbenes and acetylenes of the proposed mechanism, but there is evidence that the degradation of the BPC polymers starts with degradation of the linking group (carbonate, ester, and triazine). The presence of stilbenes and acetylenes intermediates is inferred from the MS data of the partially decomposed polycarbonate. Thermal analysis and semiempirical calculations also provide indirect evidence for the proposed mechanism, including an exothermic reaction assigned to the acetylene and the associated high char yield for BPC-based polymers. There is no evidence for direct crosslinking and charring through the dichloroethylene group. Instead, crosslinking is thought to occur through polymerization of the ethynyl degradation intermediate.

The 1,1-dichloro-2,2-bis (4-hydroxyphenyl) ethylene group can be used to increase the fire resistance of polymers relative to bisphenol-A analogs without changing the chemical and physical properties of these materials.

FUTURE WORK

More polymers can be synthesized, with the 1,1-dichloro-2,2-bis (4-hydroxyphenyl) ethylene group in the backbone to increase the fire resistance. Thermal decomposition products in the solid phase can be separated using preparative HPLC and characterized by nuclear magnetic resonance (NMR) to confirm the presence of stilbenes and acetylenes in the decomposition reactions. There is some interest in studying the effect of substituting the chlorine by other nonhalogen groups on the reactivity of this bisaryl ethylene bond and the fire-resistance properties of the polymers containing this bond.

REFERENCES

1. R.E. Lyon, "Fire-Resistant Materials: Research Overview," DOT/FAA/AR-97/99, December 1997.

2. R.E. Lyon, "Fire-Resistant Materials: Progress Report," DOT/FAA Final Report. DOT/FAA/AR-97/100, November 1998.

3. D.W. Van Krevelen, 1990, *Properties of Polymers*, 3rd. ed, Elsevier, Amsterdam.

4. R.E. Lyon, "Solid-State Thermochemistry of Flaming Combustion," DOT/FAA/AR-99/56, July 1999.

5. A. L. Rusanov, "Condensation Polymers Based on Chloral and Its Derivatives," Progress Polymer Science, Vol. 19, pp. 589-662.

6. F. Luknitskii, Chemical Reviews, Vol. 75 (3), 1975, p. 259.

7. M. Ter Meer, Ber, Vol. 7, 1874, p. 1200.

8. M. Trojna and J. Hubacek, Chem Listy, Vol 51, 1957, p. 752.

9. M. R. Mc-Laury, A. D. Chen, A.M. Colley, A. Saracino, and A.M. Tothaker, Journal of Polymer Sciences, Polymer Chemistry Edition, Vol. 18, 1980, p. 2501.

10. W. K. S. Cleveland, J. L. Webb, and C. M. Orlando, U. S. Patent 7018, 1978.

11. P.I. Kinsen and C.B. Quinn, U.S. Pat. 7,073,814, 1978.

12. W.K.S. Cedered, J.L. Webb, and C.M. Orlando, U.S. Patent 4221901, 1980.

13. T. Suzuki, T. Sonoda, S. Kobayashi, and H. Taniguchi, "Photochemistry of Vinyl Bromides: A Novel 1,2-aryl Group Migration, Journal of the Chemical Society Communication, 1975.

14. B. Sket, M. Zupan, and A. Pollak, "The Photo-Fritsch-Buttenberg-Wielchell Rearrangement," Tetrahedron, No. 10, 1976, pp. 783-784.

15. Z. Brzozowski, S. Porejko, J. Kaczorowski, and J. Kielkiewicz, U.S. Patent 3,856,566, 1974.

16. A. Factor, M.R. MacLaury, and J.L. Webb, U.S. Patent 4,097,538, 1978.

17. A. Factor and C.M. Orlando, "Polycarbonates From 1,1-Dichloro-2,2-Bis(4-Hydroxyphenyl)Ethylene and Bisphenol A: A Highly Flame-Resistant Family of Engineering Thermoplastics," Journal of Polymer Sciences, Polymer Chemistry Edition, Vol. 18, 1980, pp. 579-592.

18. Z. Wielgosz, Z. Boranowska, and K. Janicka, "Infrared Spectroscopic Investigation of Polycarbonates," Plaste und Kautschuk, Vol. 19, 1972, pp. 902-904.

19. C.B. Quinn, "The Flammability Properties of Copolyesters and Copolycarbonates Containing Acetylenes," Journal of Polymer Sciences, Polymer Chemistry Edition, Vol. 15, 1977, pp. 2587-2594.

20. A.S. Politou, C. Morterra, and M.J.D. Low, "Infrared Studies of Carbons; the Formation of Chars From a Polycarbonate," Carbon, Vol. 28 No.4, 1990, pp. 529-538.

21. G. Montaudo and C. Puglisi, "Thermal Degradation Mechanisms in Condensation Polymers," in N. Grassie (ed), *Developments in Polymer Degradation*, Vol. 7, Chapter 2, Elsevier Applied Science, London, UK, 1987, pp. 35-81.

22. S. L. Madorski, *Thermal Degradation of Organic Polymers*, Chapter 16, International Science Publishers, New York, USA, 1964, pp. 293-303.

23. H. Schnell, *Chemistry and Physics of Polycarbonates*, John Wiley and Sons, USA, 1964.

24. J.R. Stewart, "Synthesis and Characterization of Chlorinated Bisphenol-Based Polymers and Polycarbodiimides as Inherently Fire-Safe Polymers," DOT/FAA/AR-00/39, August 2000.

25. W.W. Wendlandt, *Thermal Methods of Analysis*, second edition, John Wiley & Sons, USA, 1974.

26. R.E. Lyon, "An Integral Method of Nonisothermal Kinetic Analysis," Termochimica Acta, 297, 1997, pp. 117-124.

27. D.W. Van Krevelen, "Some Basic Aspects of Flame Resistance of Polymeric Materials," Polymer, Vol. 16, 1975, pp. 615-620.

28. http://www.scimedia.com/chem-ed/sep/lc/ion-chro.htm.

29. E. Sawiki, J, D. Malic, and Ewittbenstein, *Ian Chrantegraphic Analysis of Enviromental Polutants*, 1st edition, 1978.

30. H. W. Siesler and K. Holland-Moritz, *Infrared and Raman Spectroscopy of Polymers*, 1st edition, Ana Harsor Science, 1980.

31. B. C. Smith, *Fundamentals of Fourier Transform Infrared Spectroscopy*, CRC Press, New York, 1996.

32. http://www.cicp.com/ftir.html#hotone, Active, January 2000.

33. Frank Cheng–Yu Wang and Patrick B. Smith, "Compositional and Structural Studies of Vinylidene Chloride Copolymers by Pyrolysis Gas Chromatography," Analytical Chemistry, Vol. 68. No. 6, 1996, pp. 425-430.

34. Frank Cheng–Yu Wang, Bruce B. Gerhart, and Patrick B. Smith, "Structure Determination of Polymeric Materials By Pyrolysis Gas Chromatography," Analytical Chemistry, Vol. 67 No. 19, 1995, pp. 3636-3640.

35. Frank Cheng-Yu Wamg. "Polymers Degradation Mechanism Reselection Through Derivatization for Qualitative Pyrolysis Gas Chromatography Analysis," Analytical Chemistry, Vol. 70. No.17, 1998, pp. 3642-3648.

36. A. Davis and H. Golden J., Macromolecular Sciences Reviews Macromolecular Chemistry, Vol. 3, 1969, p. 49.

37. D.A. Gallagher, "Computer-Aided Chemistry Techniques Reveal Thermal Degradation Mechanisms of Polymers," Scientific Computing and Automation, June 1996.

38. J. J. Stewart, "Semiempirical Molecular Orbitals Methods," in K. B. Kiptowitz and B. B. Boyd (eds), *Reviews in Computational Chemistry*, VCH Publisher, USA, Chapter 2, 1990, p. 45.

39. J. J. Stewart, Journal of Computational Chemistry, Vol. 10 (2), 1989, p. 229.

40. J. J. Stewart, "MOPAC Program Version 6" Quantum Chemistry Program Exchange, University of Indiana, adapted and modified by CaChe Scientific, USA.

41. A. Factor, "Char Formation in Aromatic Engineering Polymers," in Nelson, G.L.(ed), *Fire and Polymers, Hazards Identification and Prevention*, Chapter 19, ACS Publishing, Washington, D.C., 1990, pp. 274-287.

42. J.A. Hinkley, "DSC Study of the Cure of a Phenyl-Terminated Imide Oligomers," Journal of Advanced Materials, April 1996, pp. 55-59.

43. A.W. Snow, "The Synthesis, Manufacture and Characterization of Cyanate Ester Monomers," in I. Hamerton, *Chemistry and Technology of Cyanate Ester Resins*, first edition, chapter 2, 1994, pp. 7-54.

44. R. M. Silverstein, G. Clayton, and T. Morrill, *Spectrometric Identification of Organic Compounds*, third edition, John Wiley and Sons, Inc., USA, 1974.

45. F.A. Miller, W.F. Elbert, and W. Pingitore, Journal of Molecular Structures, Volume 41, 1977, p. 19.

46. D. A. Shimp, J. R. Christenson, and S. J. Ising, 34th International SAMPE Exhibition, Vol. 34, 1989, p. 222.

47. V. V. Korshak, P. N. Gribkova, A. V. Dmitrienko, and S. V. Vinogradova, Vysokomol. Soed., Vol. A16, 1974, p. 14.

48. D. A. Shimp and S. J. Ising, *American Chemical Society National Meeting PMSE Division,* San Francisco, California, ACS Press, Washington, D. C., April 1992.

49. B A. Howell, "The Application of Thermogravimetry for the Study of Polymer Degradation," Thermochimica Acta, 148, 1989, pp. 375-380.

ADDITIONAL INFORMATION

D. Lin-Vien, N.B. Colthup, W.G. Fateley, and J.G. Grasselli, *The Handbook of Infrared and Raman Characteristic Frequencies of Organic Molecules*, Academic Press Inc., San Diego, California, 1991.

Craig L. Beyler and Marcelo M. Hirshler, *Thermal Decomposition of Polymers*, Handbook of Fire Protection Engineering, 1994, pp. 99-117.

Richard E. Lyon, 1996, "Fire-Safe Aircraft Cabin Materials," Fire and Polymers, Symposium, ACS National Meeting, Washington, DC, August 1994, pp. 599-638.

Richard E. Lyon, "FAA Research in Fire Safety Materials," Journal of the Society for the Advancement of Materials and Process Engineering, Vol. 41-I, 1996, pp. 334-345.

http://www.cdsanalytical.com/prodframe.htm, active January 2000.

F. W. Billmeyer, 971, *Textbook of Polymer Science*, second edition, Wiley-Interscience Inc., New York, USA.

R.E. Lyon, "Pyrolysis Kinetics of Char Forming Polymers," Polymer Degradation and Stability, Vol. 61, 1998, pp. 201-210.

J. Troitzch, *International Plastics Flammability Handbook*, 2nd edition, Hanser Publisher, New York, 1990.

B. S. Furniss, A. J. Hannaford, P. W. G. Smith, and A. R. Tatchell, *Vogel's Textbook of Practical Organic Chemistry*, fifth edition, Longman Scientific and Technical, Great Britain, 1991, p. 1257.

J. March, *Advanced Organic Chemistry*, third edition, John Wiley and Sons, New York, 1985, pp. 329-331.

H. Shnell, "Industrial Engineering Chemistry," Vol. 51, 1959, p. 157.

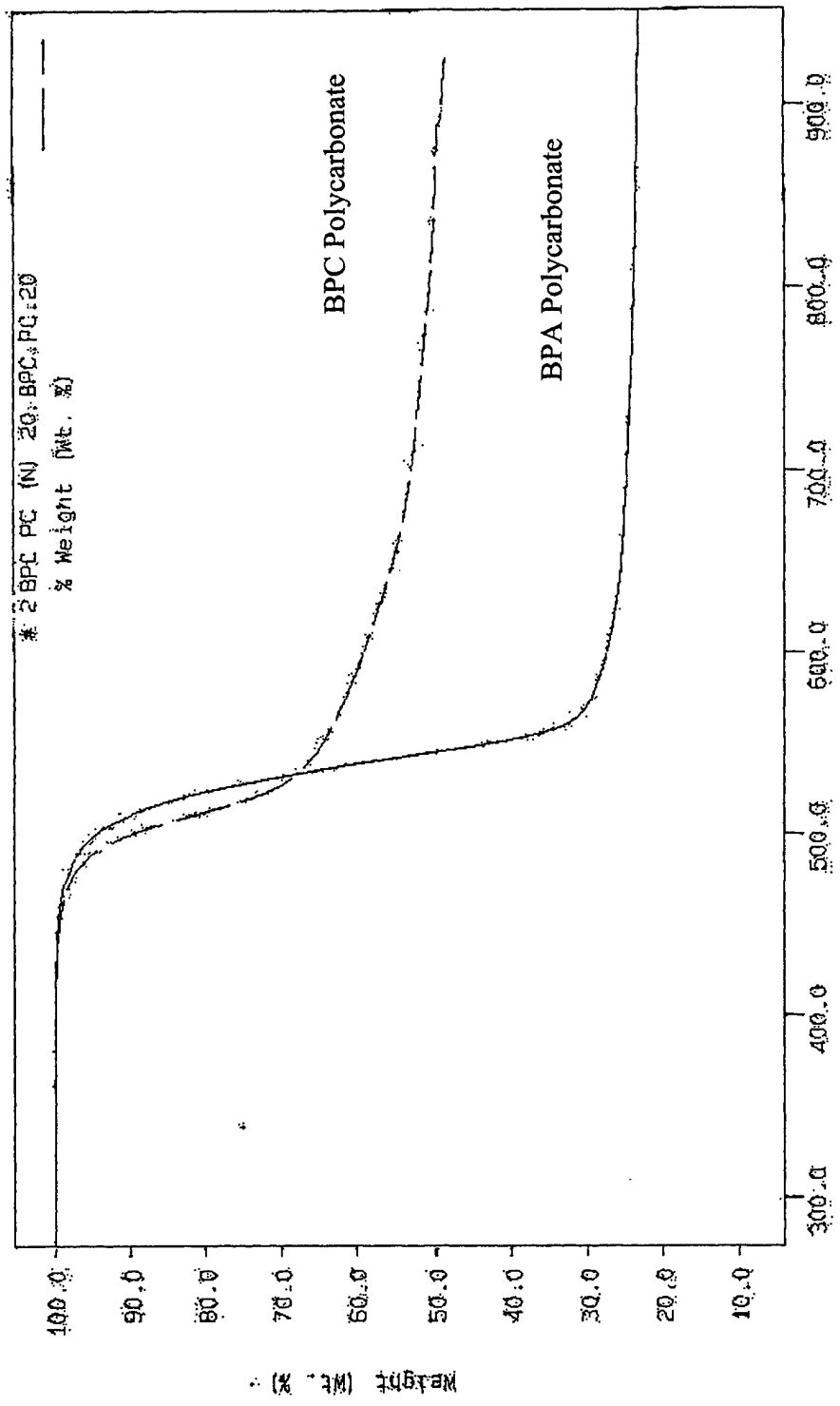

FIGURE A-1. TGA OF BPC AND BPA POLYCARBONATES

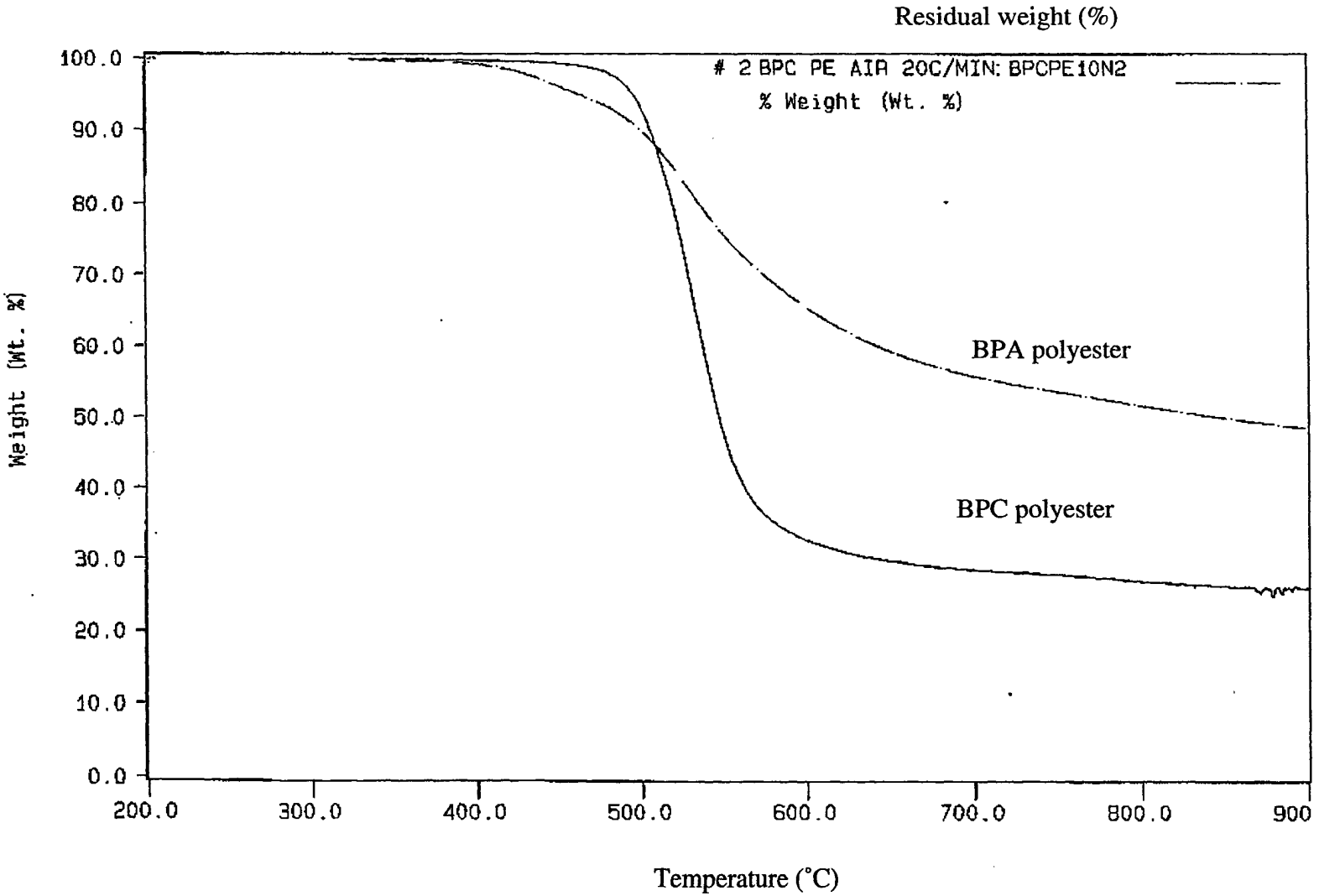

FIGURE A-2. TGA CURVES OF BPA AND BPC POLYESTERS

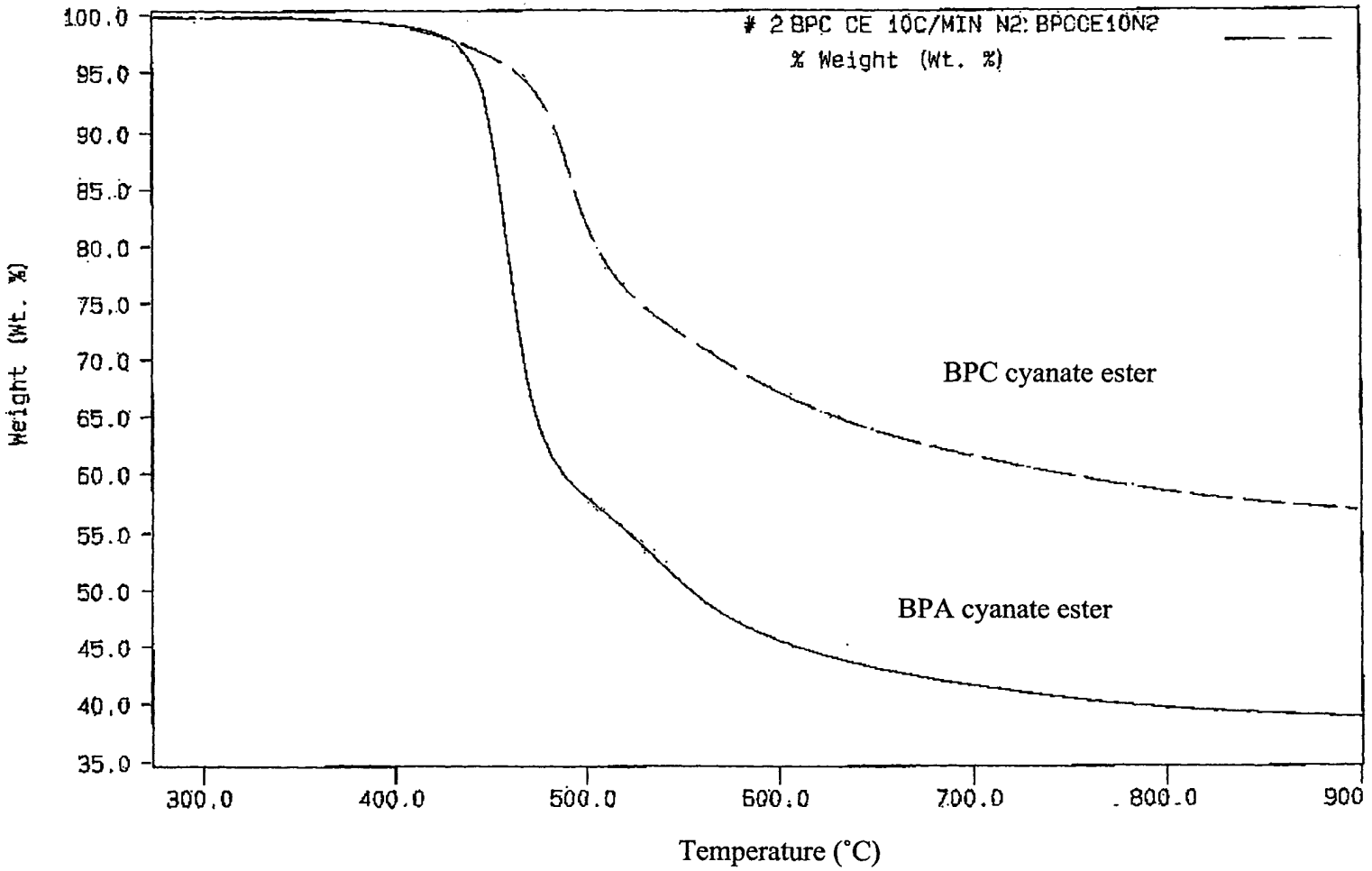

FIGURE A-3. TGA OF BPC AND BPA CYANATE ESTERS

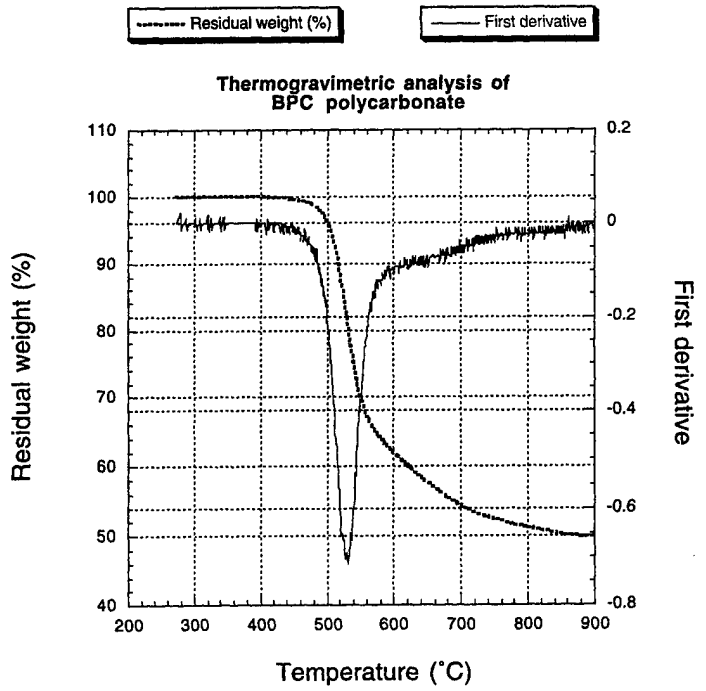

FIGURE A-4. TGA OF BPC POLYCARBONATE

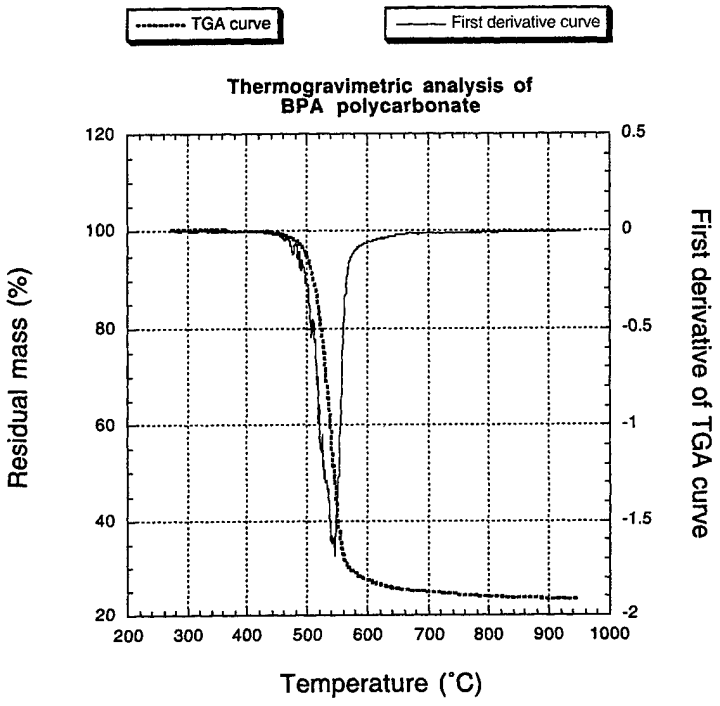

FIGURE A-5. TGA OF BPA POLYCARBONATE

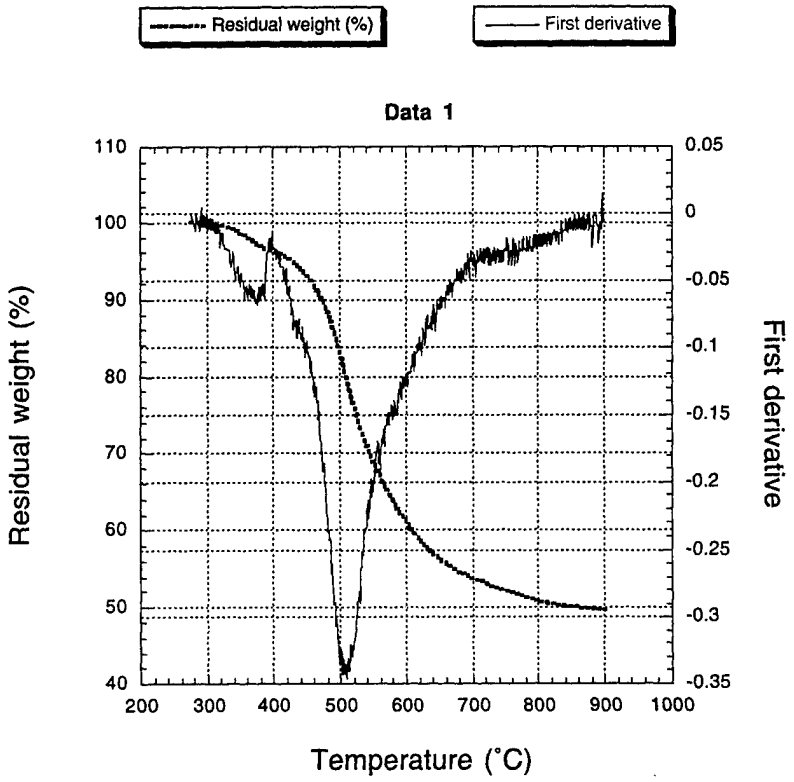

FIGURE A-6. TGA OF BPC POLYESTER

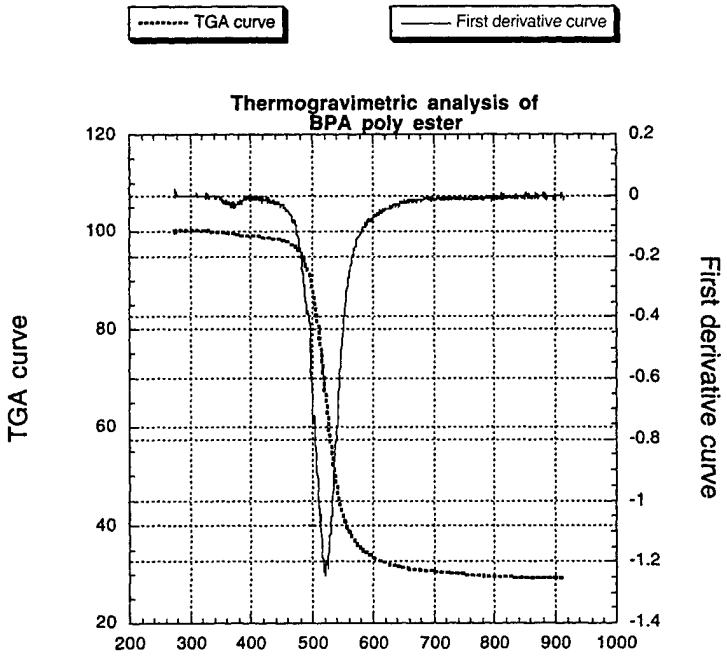

FIGURE A-7. TGA OF BPA BASED POLYESTER

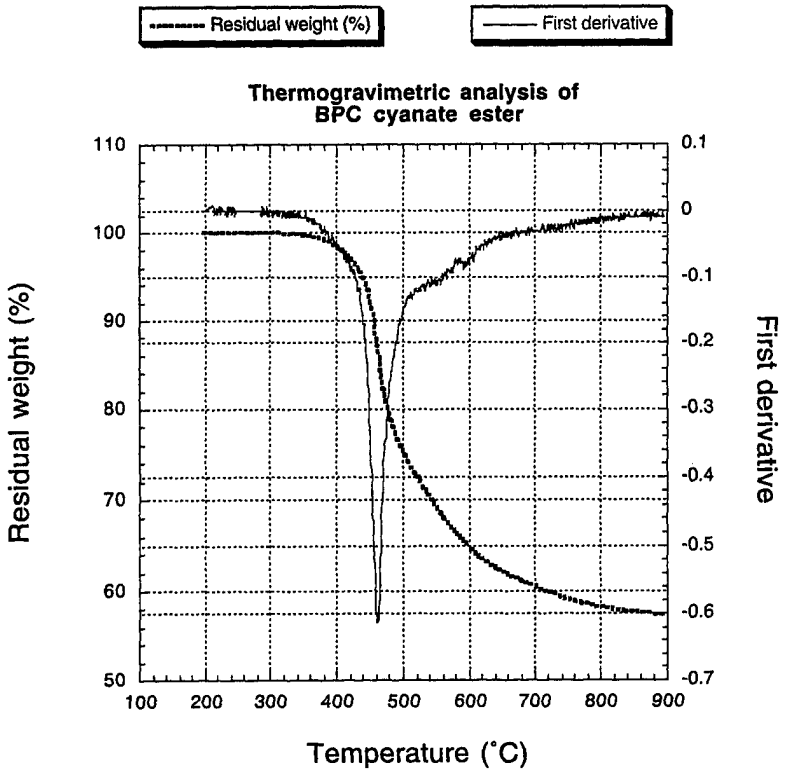

FIGURE A-8. TGA OF BPC CYANATE ESTER

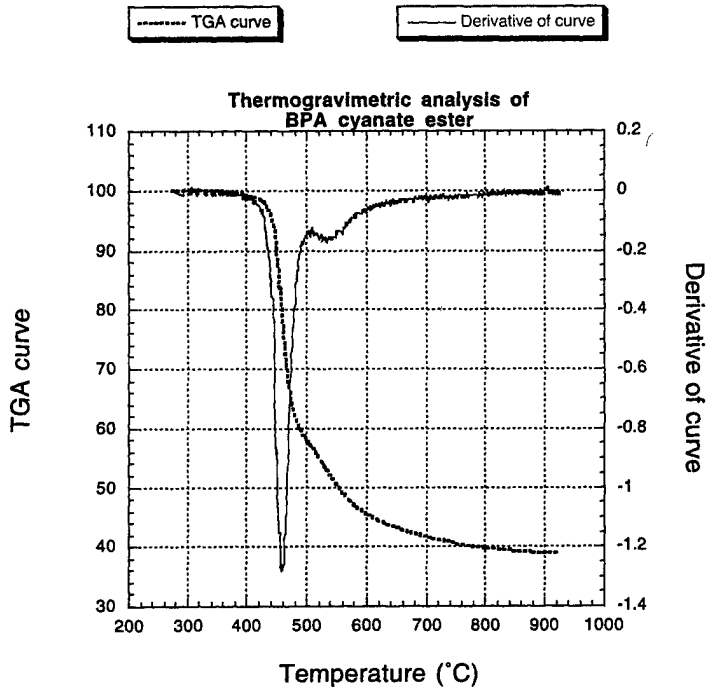

FIGURE A-9. TGA OF BPA CYANATE ESTER

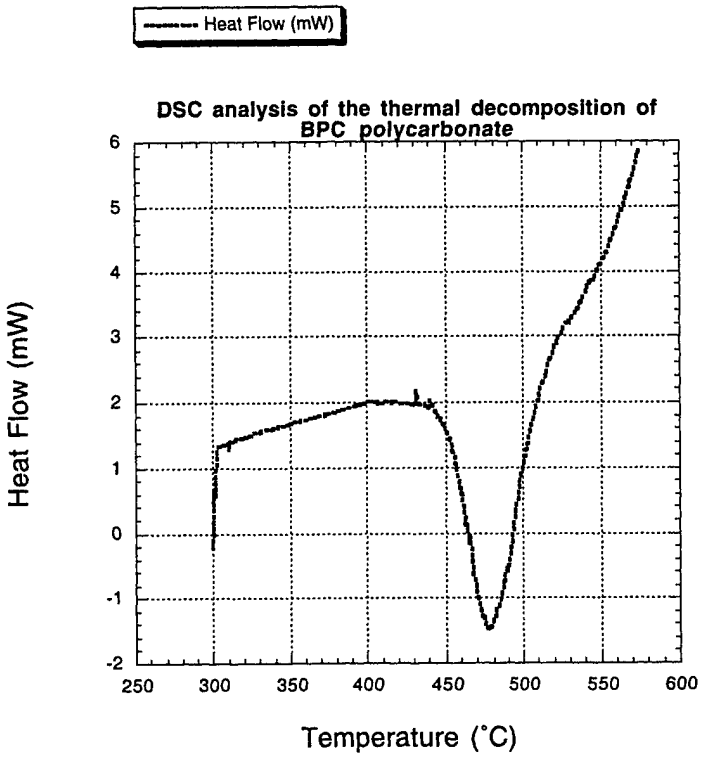

FIGURE A-10. DSC OF BPC POLYCARBONATE

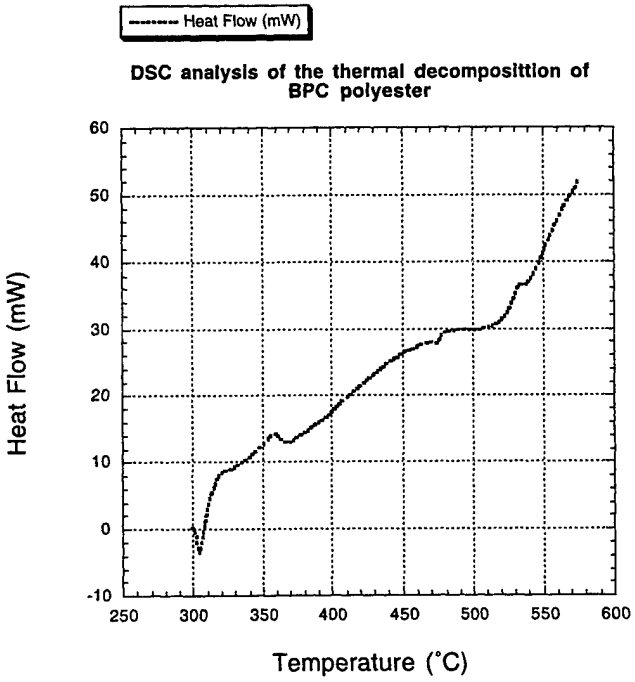

FIGURE A-11. DSC OF BPC POLYESTER

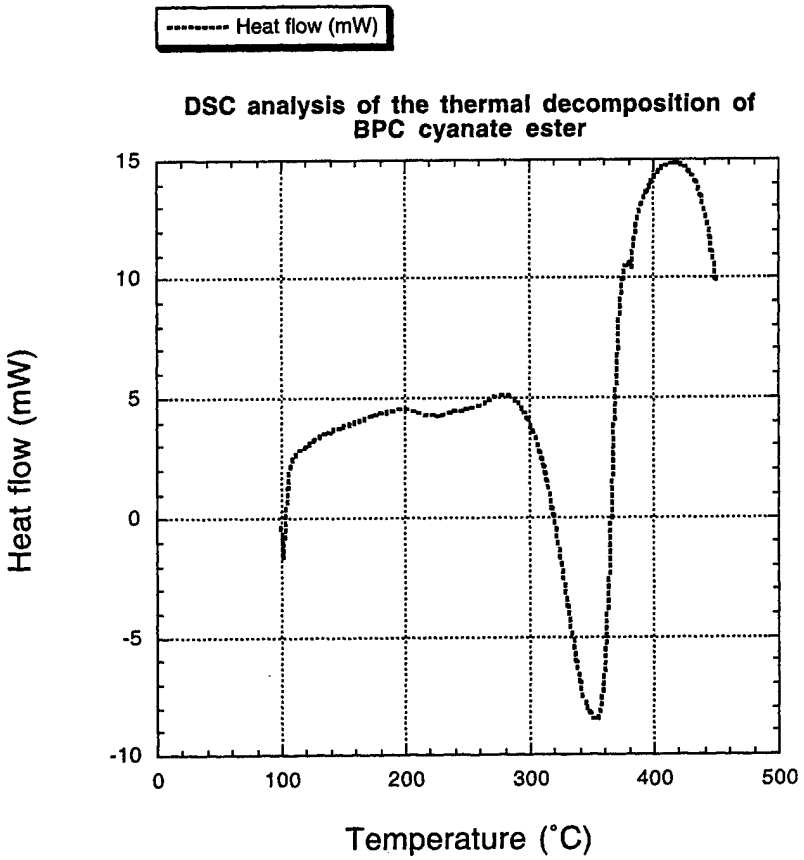

FIGURE A-12. DSC OF BPC CYANATE ESTER

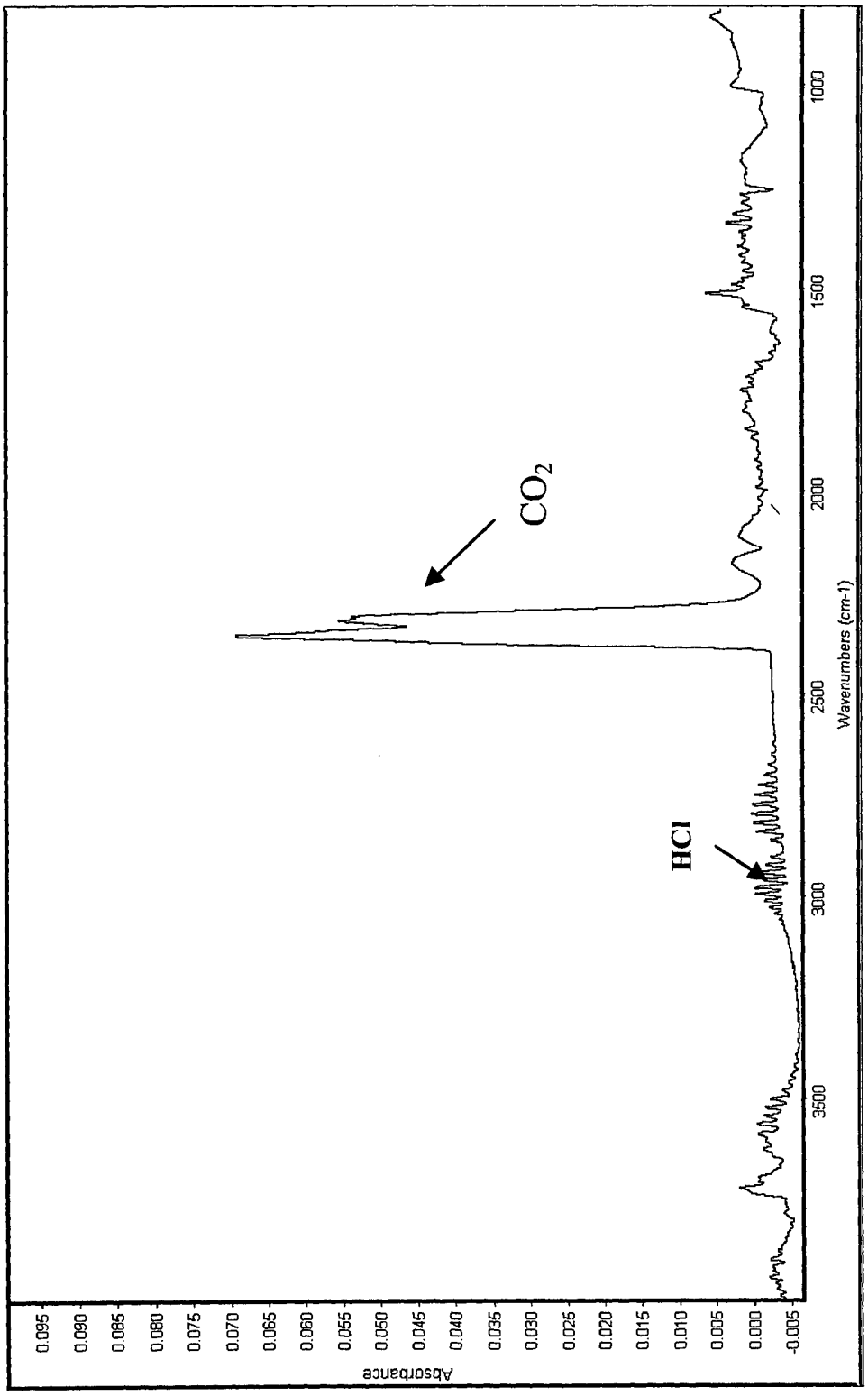

FIGURE B-1. IR OF BPC-BASED POLYCARBONATE GASEOUS DECOMPOSITION PRODUCTS

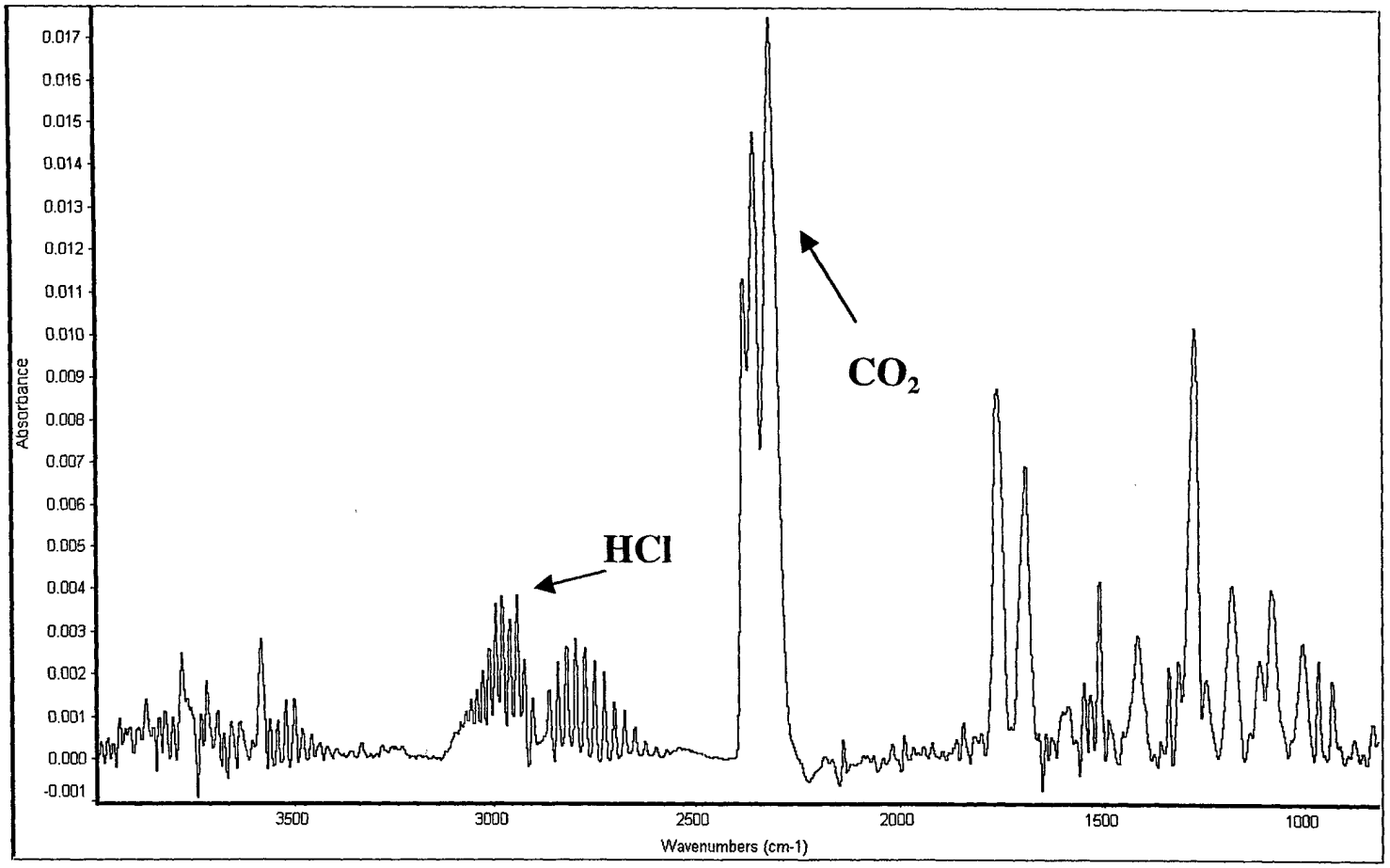

FIGURE B-2. IR OF THE GASEOUS DECOMPOSITION PRODUCTS OF BPC-BASED POLYESTER

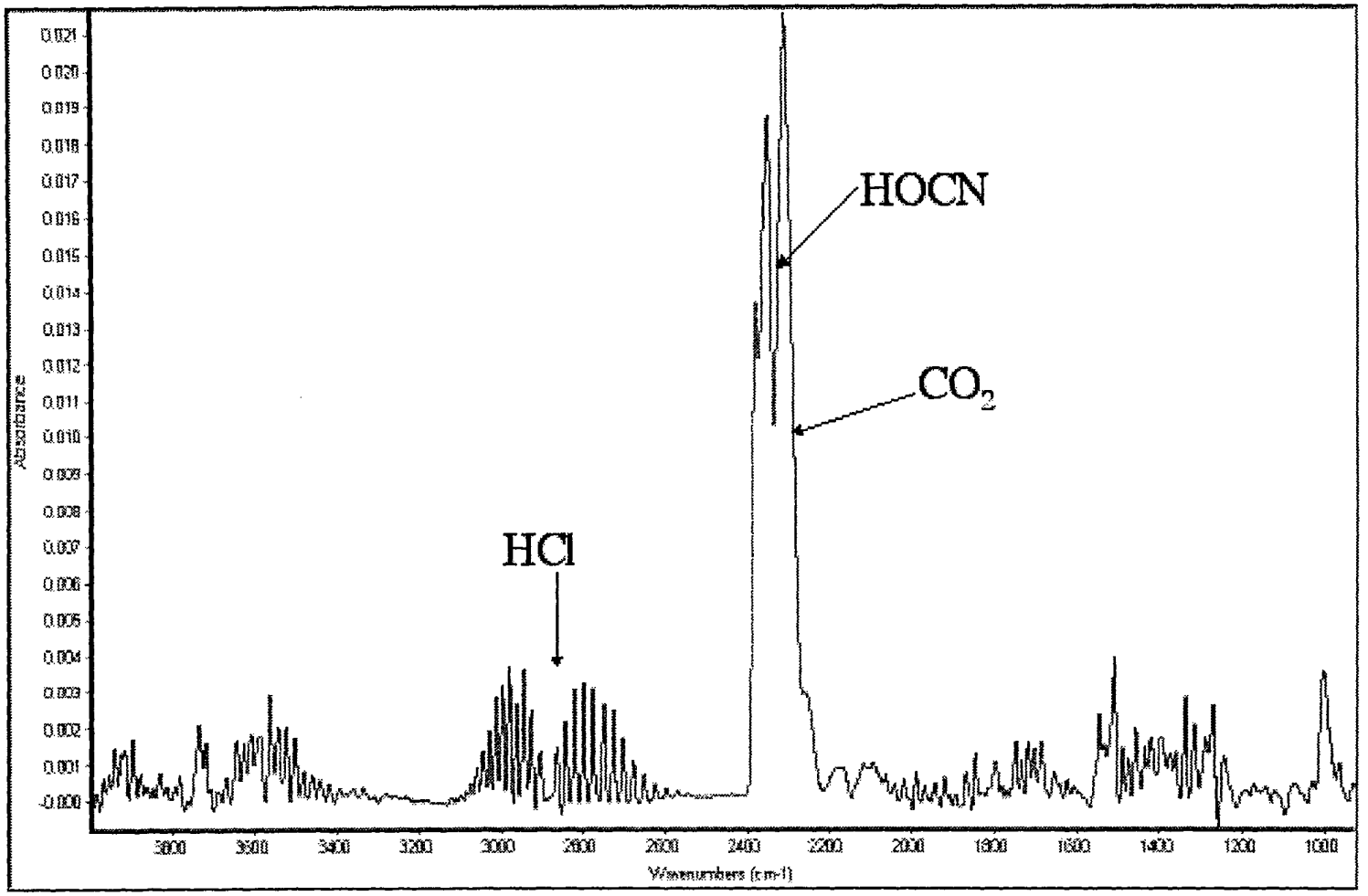

FIGURE B-3. IR OF THE GASEOUS DECOMPOSITION PRODUCTS OF BPC-BASED CYANATE ESTER

APPENDIX C—MASS SPECTRA OF PYROLYSIS PRODUCTS

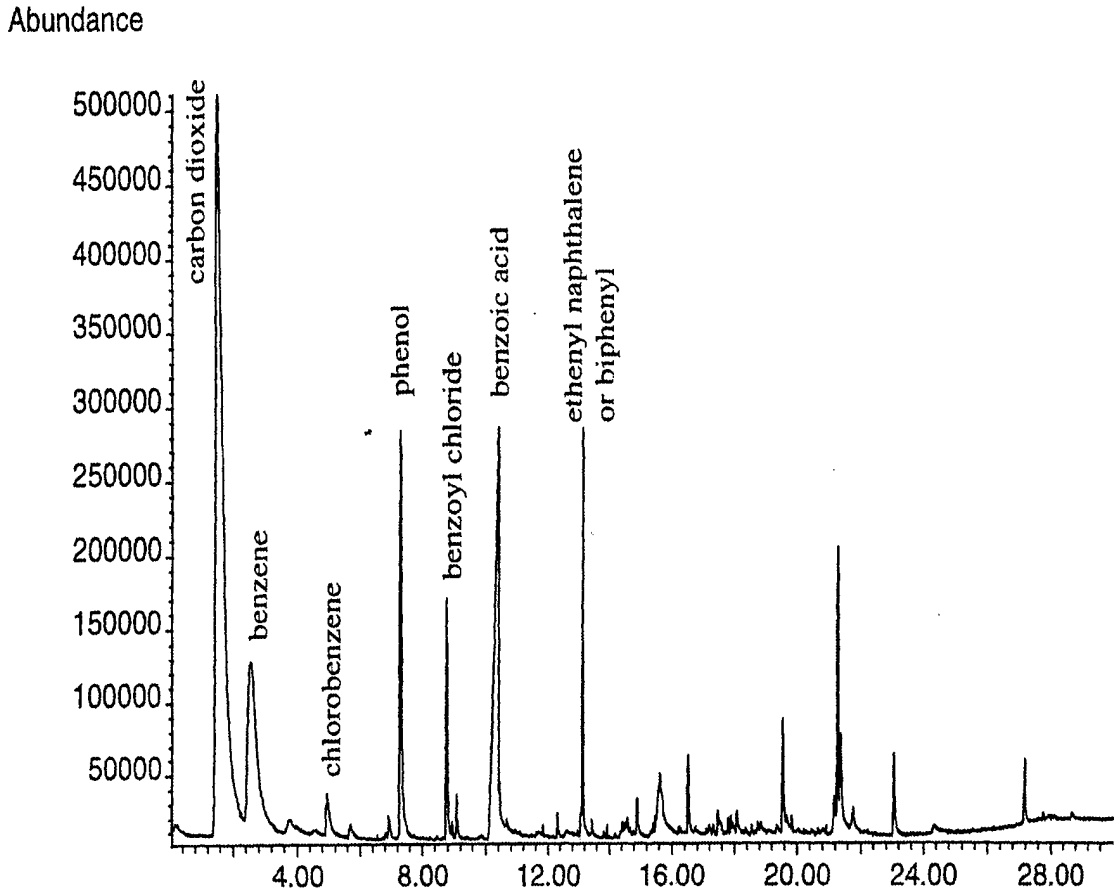

FIGURE C-1. PY-GC MS ANALYSIS OF BPC-BASED POLYESTER

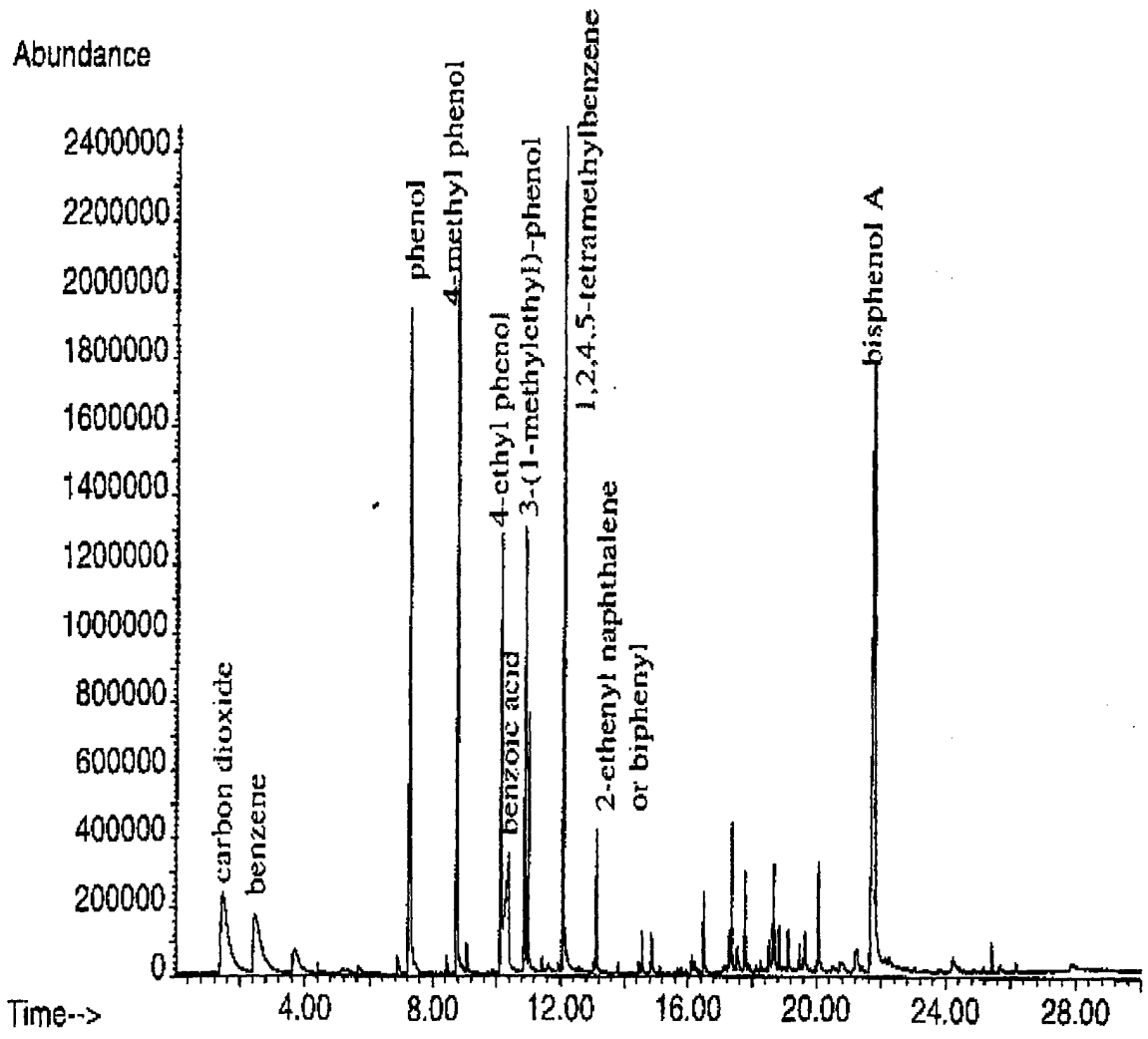

FIGURE C-2. PY-GC MS ANALYSIS OF BPA-BASED POLYESTER

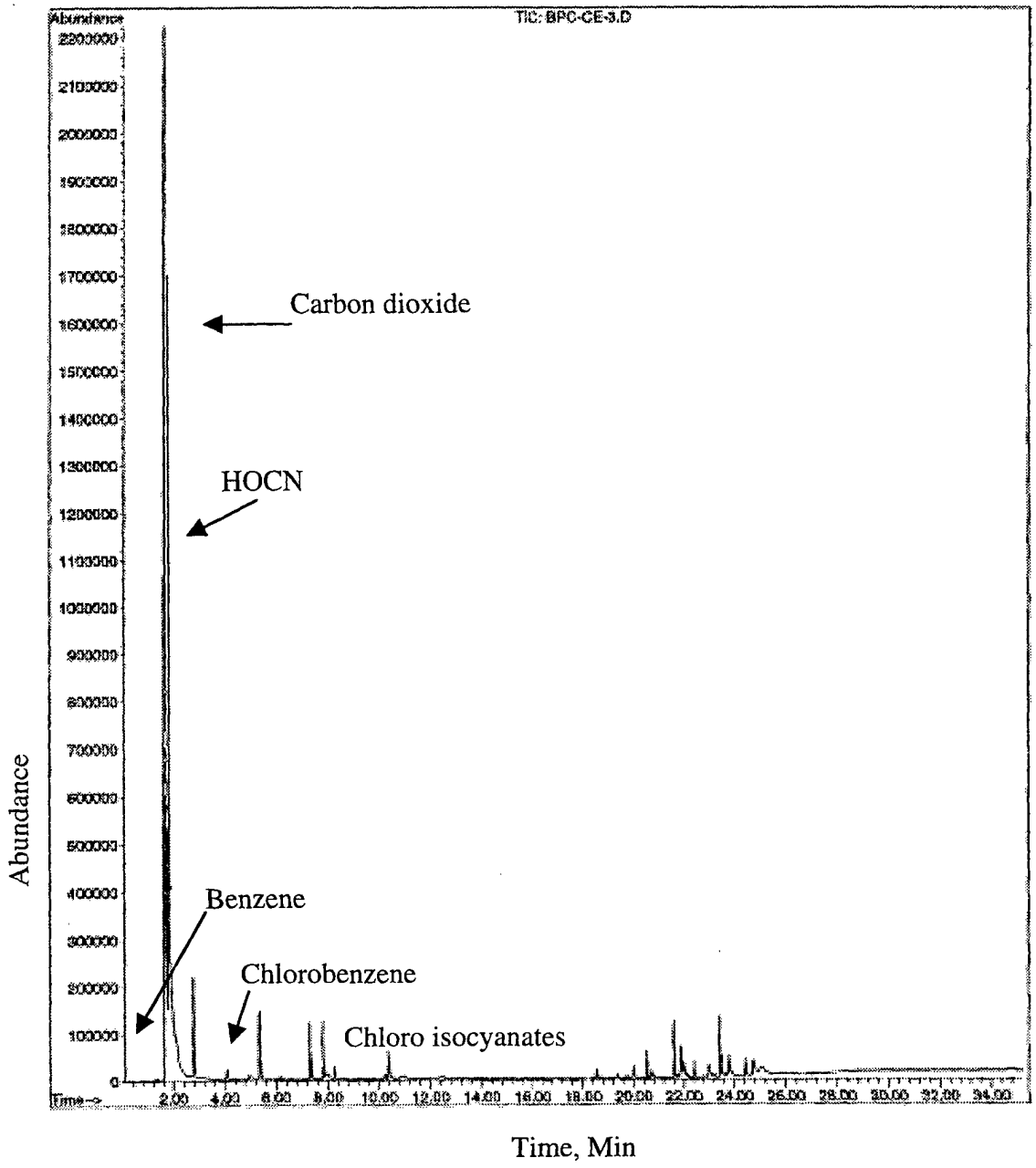

FIGURE C-3. PY-GC MS ANALYSIS OF BPC-BASED CYANATE ESTER

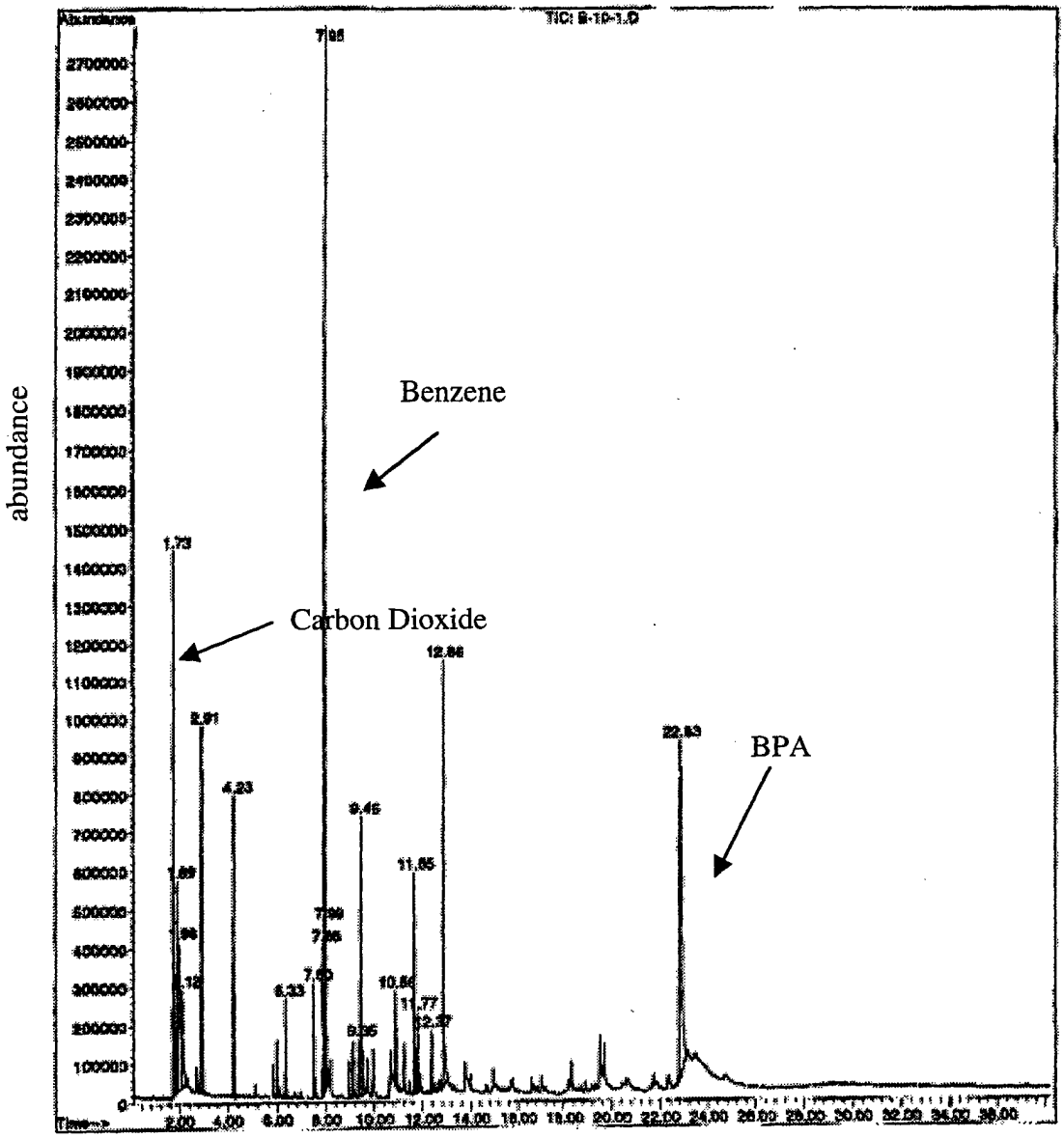

FIGURE C-4. PY-GC MS ANALYSIS OF BPA-BASED CYANATE ESTER

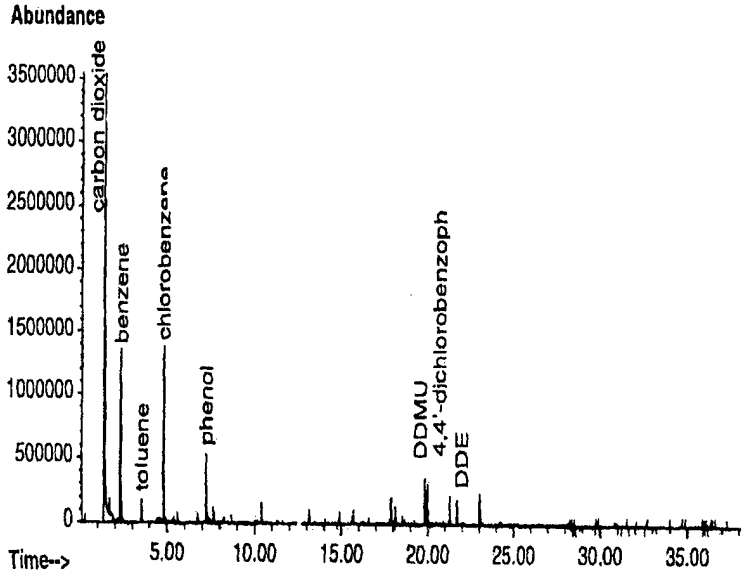

Time, Min

FIGURE C-5. PY-GC MS ANALYSIS OF BPC-BASED POLYCARBONATE

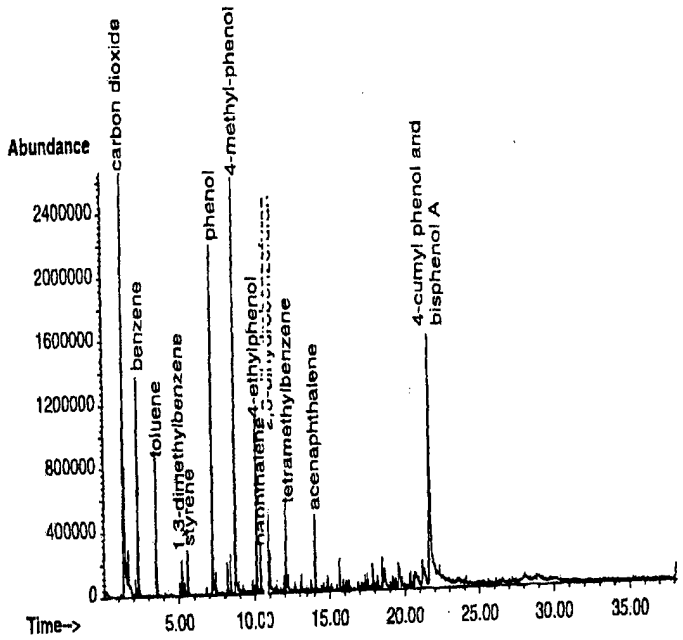

Time, Min

FIGURE C-6. PY-GC MS ANALYSIS OF BPA-BASED POLYCARBONATE

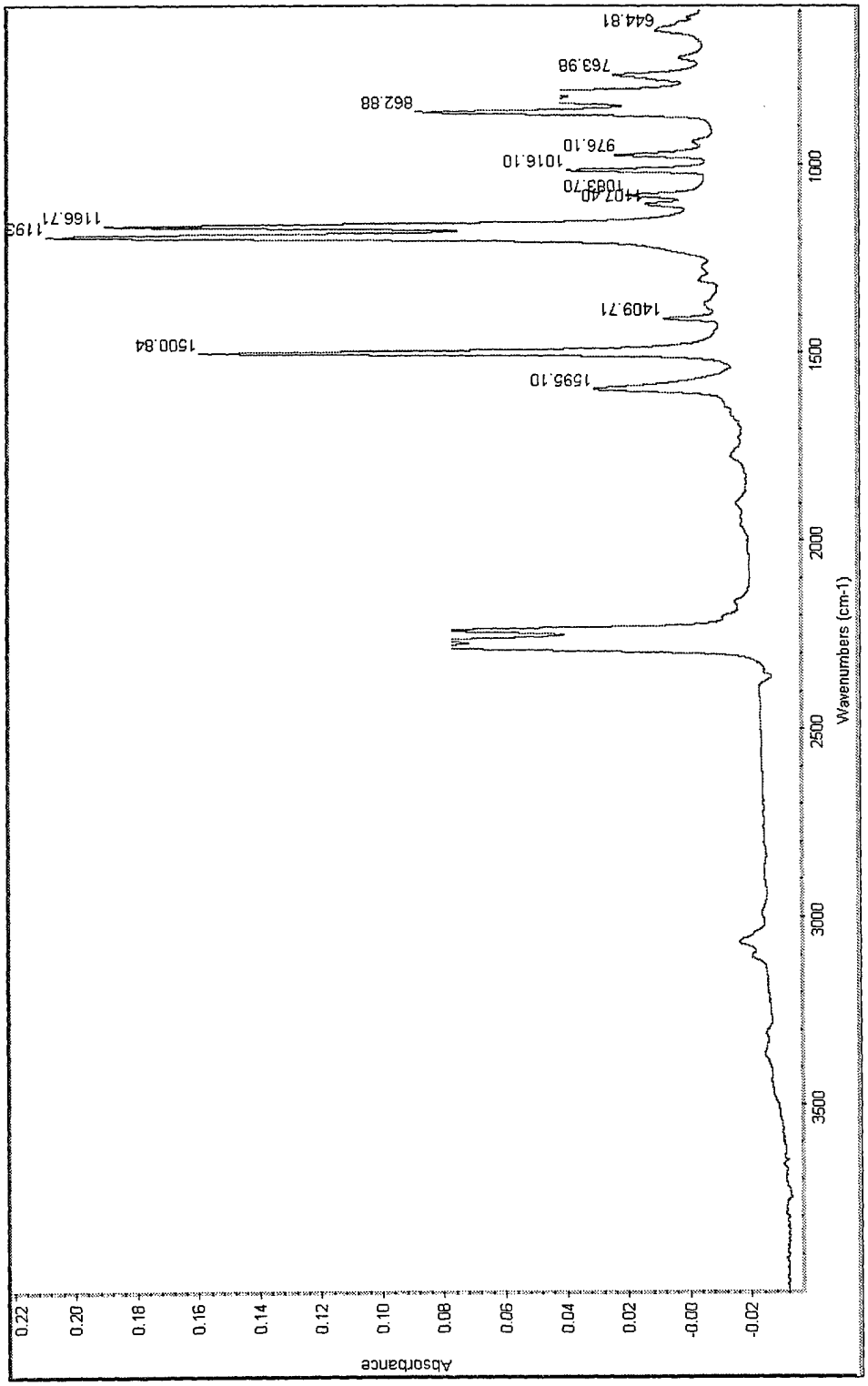

FIGURE D-1. IR SPECTRA OF UNCURED BPC-BASED CYANATE ESTER

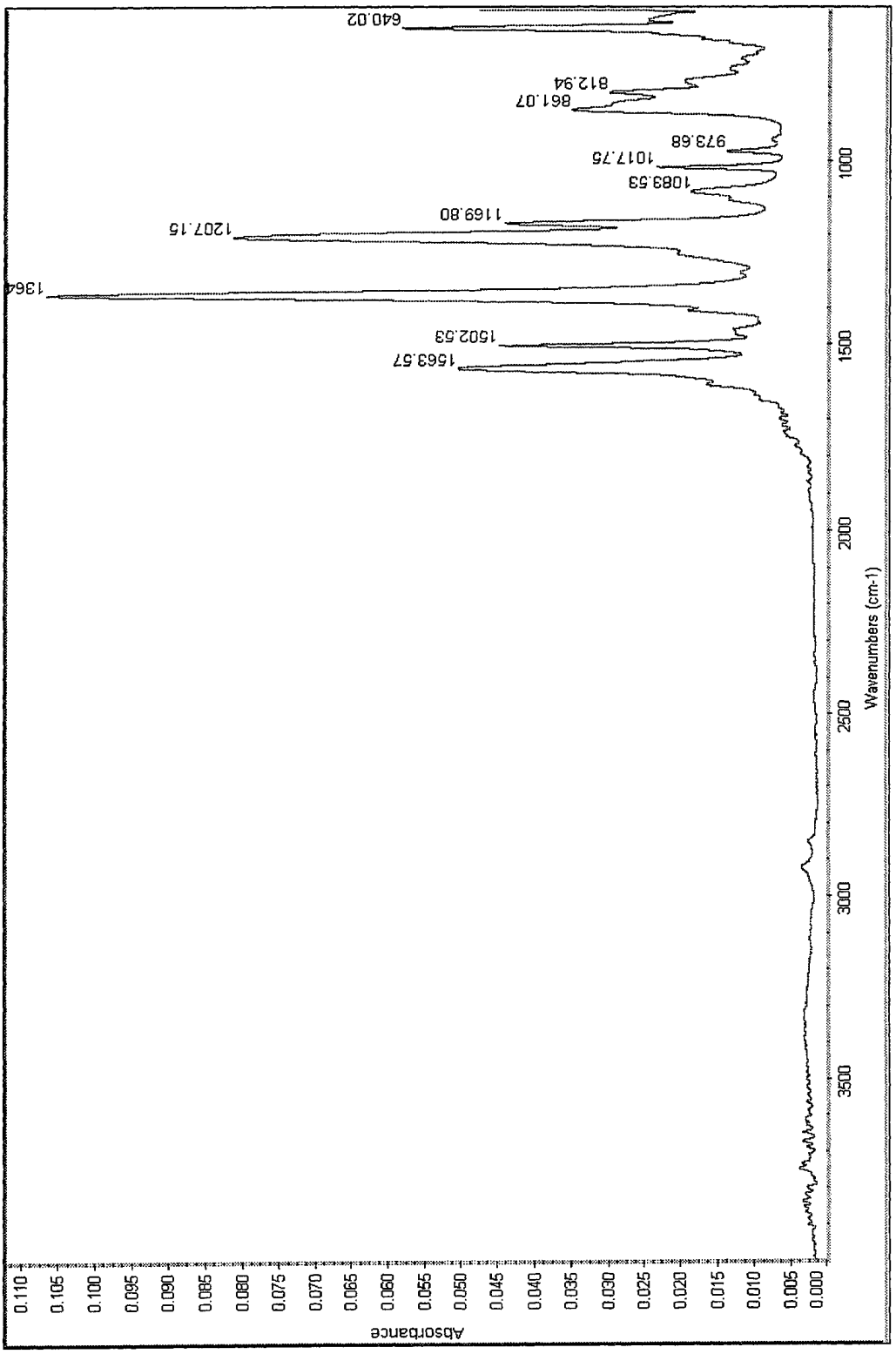

FIGURE D-2. IR SPECTRA OF CURED BPC-BASED CYANATE ESTER

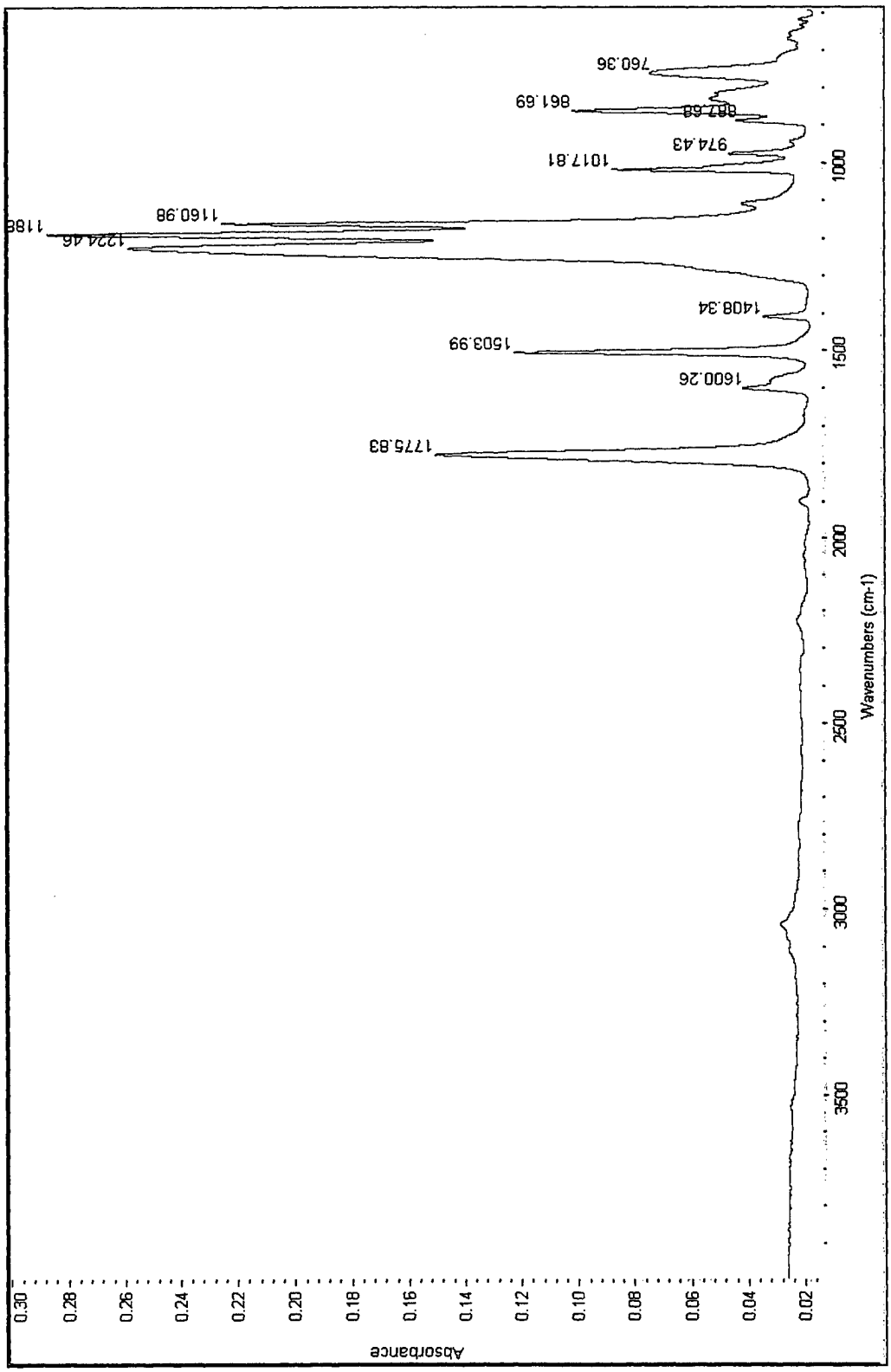

FIGURE D-3. IR SPECTRA OF BPC-BASED POLYCARBONATE

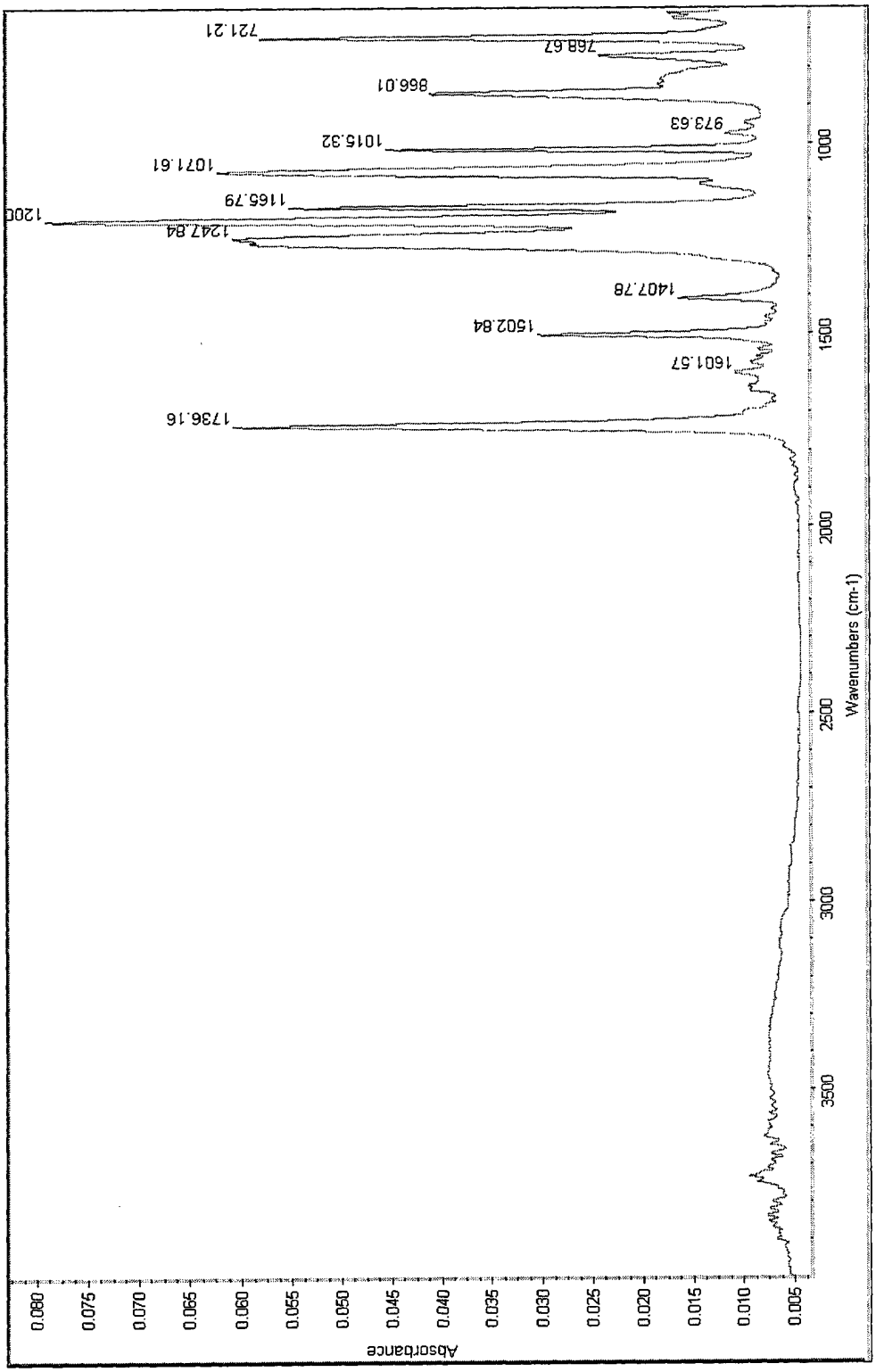

FIGURE D-4. IR SPECTRA OF BPC-BASED POLYESTER

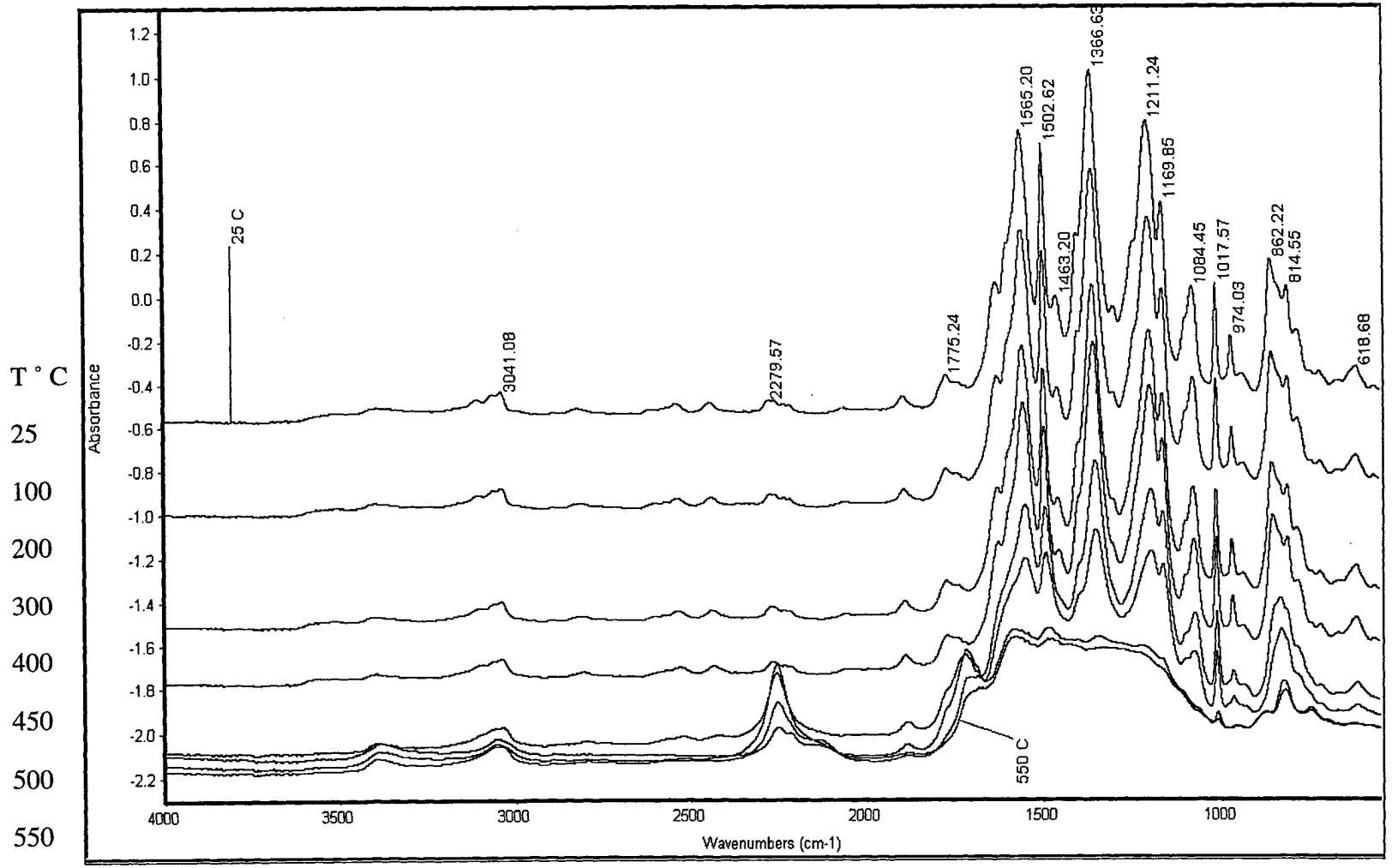

FIGURE D-5. IR SPECTRA OF THE THERMAL DECOMPOSITION OF BPC-BASED CYANATE ESTER

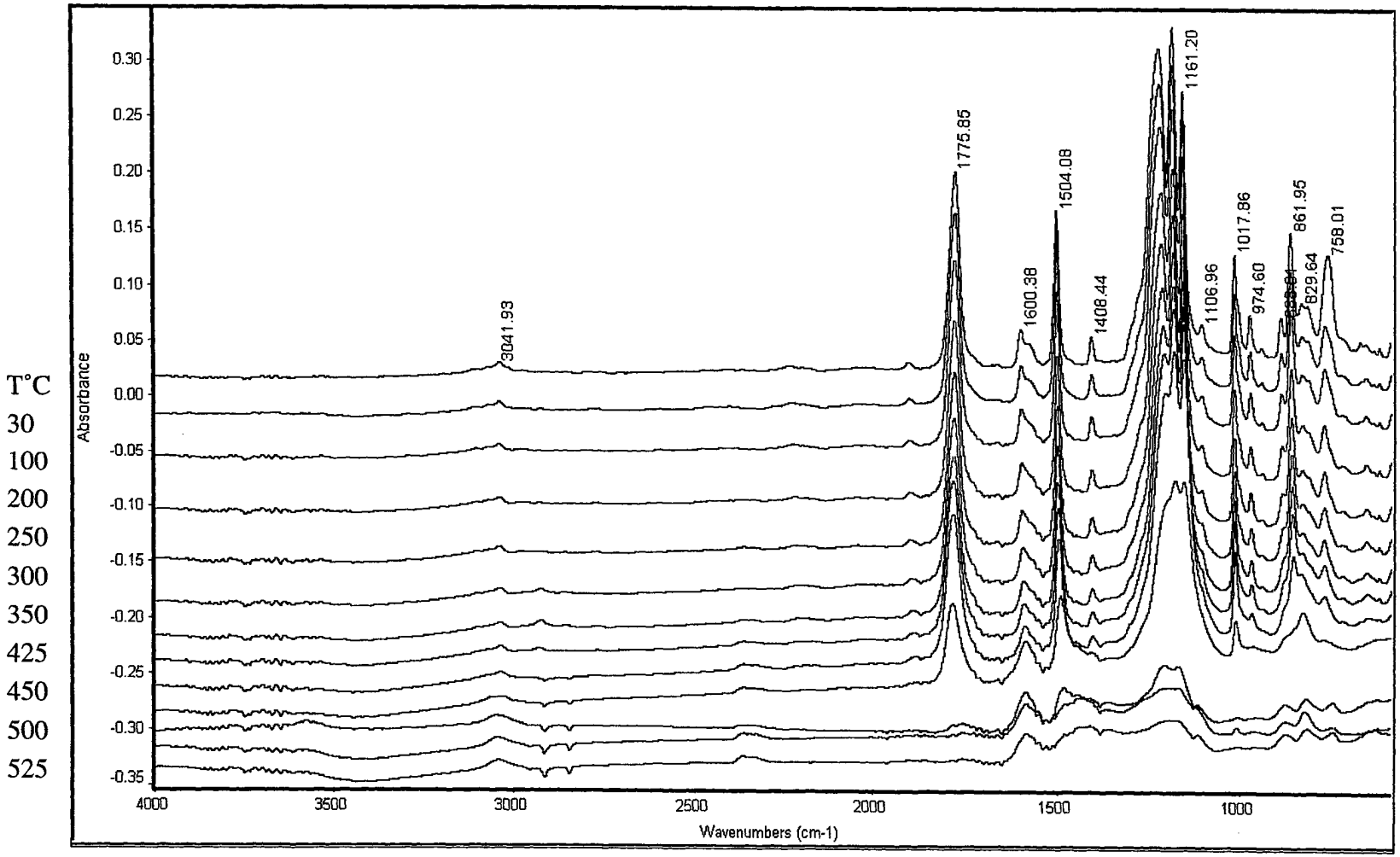

FIGURE D-6. IR SPECTRA OF THE THERMAL DECOMPOSITION OF BPC-BASED POLYCARBONATE

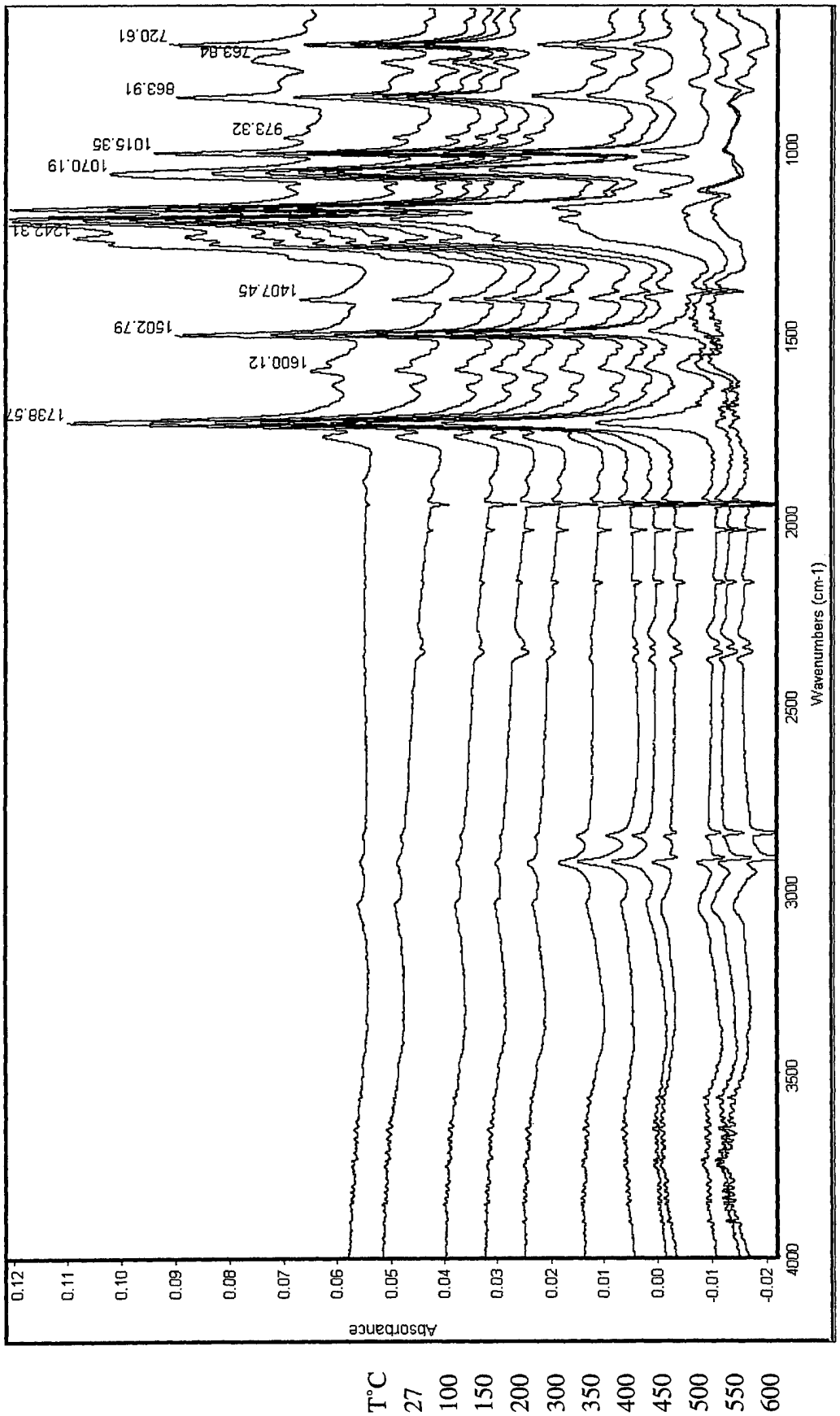

FIGURE D-7. IR SPECTRA OF THE THERMAL DECOMPOSITION OF BPC-BASED POLYESTER

APPENDIX E—STUDIES ON CROSSLINKED SAMPLES

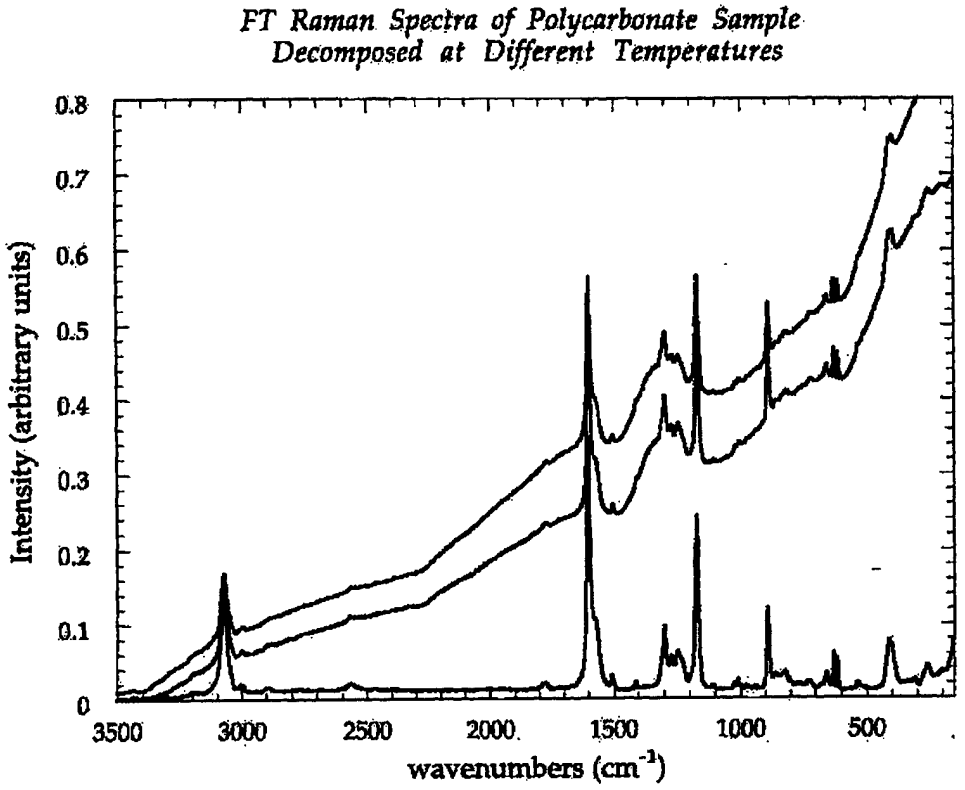

FIGURE E-1. RAMAN SPECTRA OF BPC POLYCARBONATE AT ROOM TEMPERATURE (BOTTOM) AND HEATED FOR 1 HOUR AT 300°C (MIDDLE), AND 450°C (TOP)

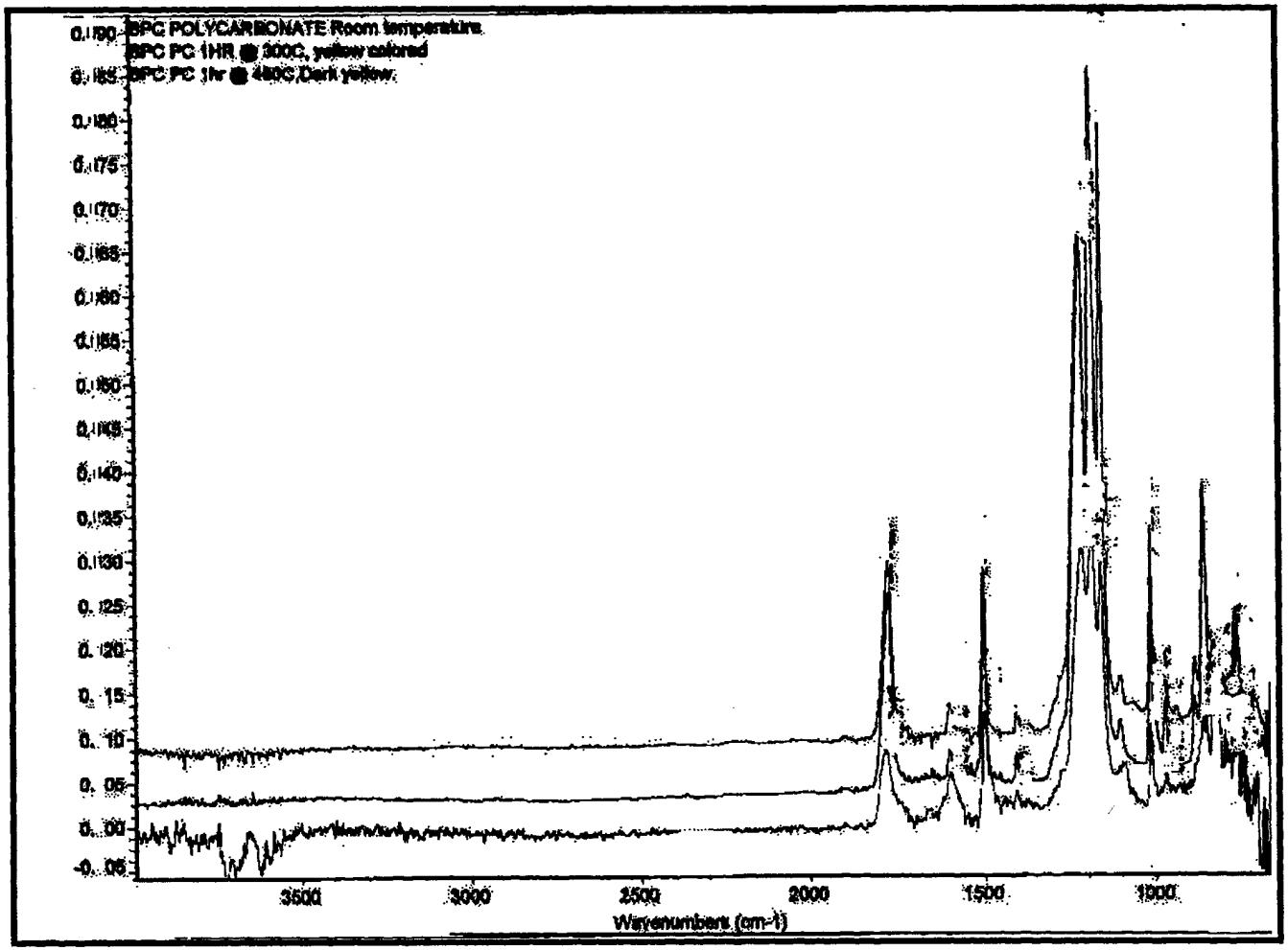

FIGURE E-2. ATR IR SPECTRA OF CROSSLINKED POLYCARBONATE SAMPLE

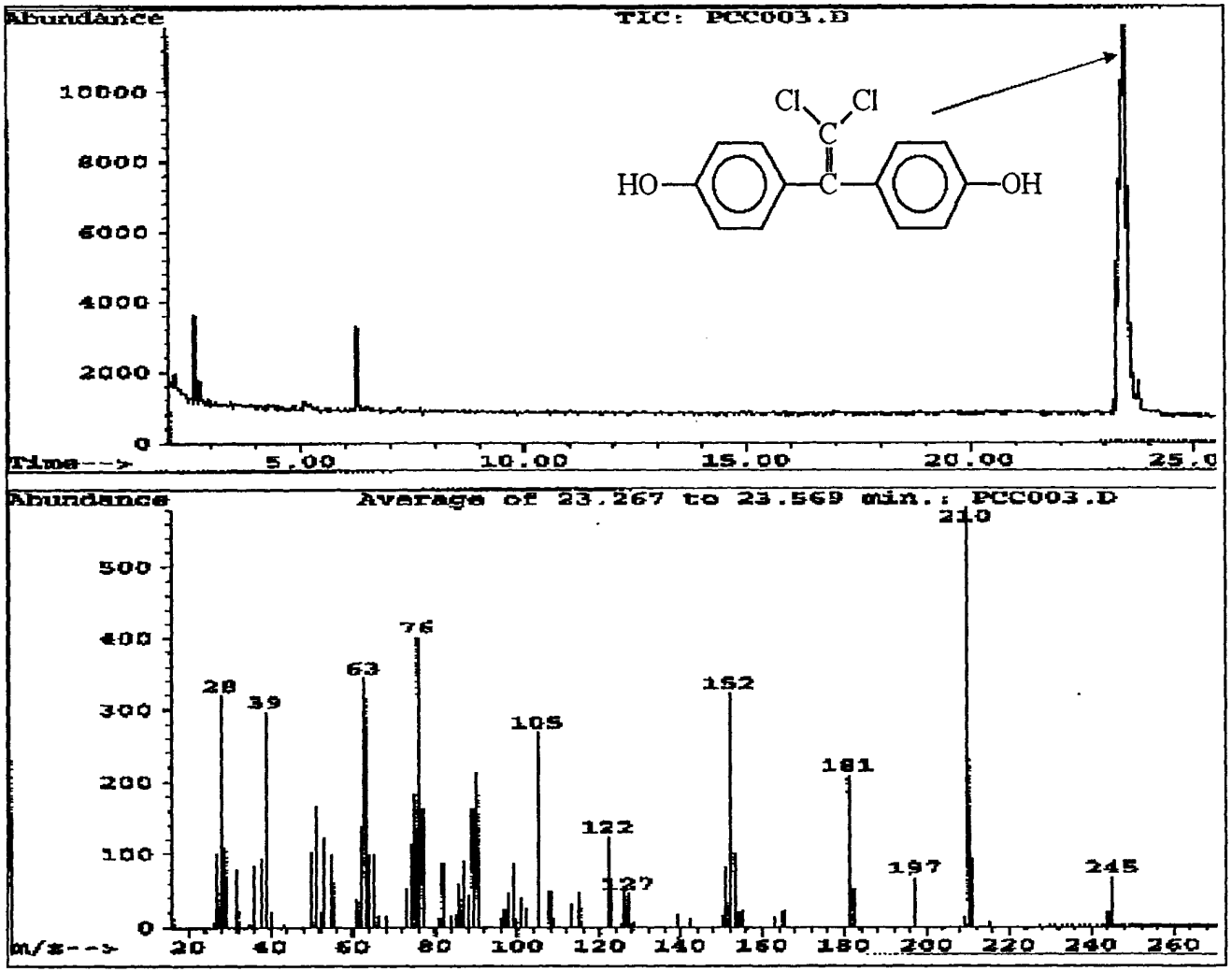

FIGURE E-3. GC MS OF BPC POLYCARBONATE AT ROOM TEMPERATURE

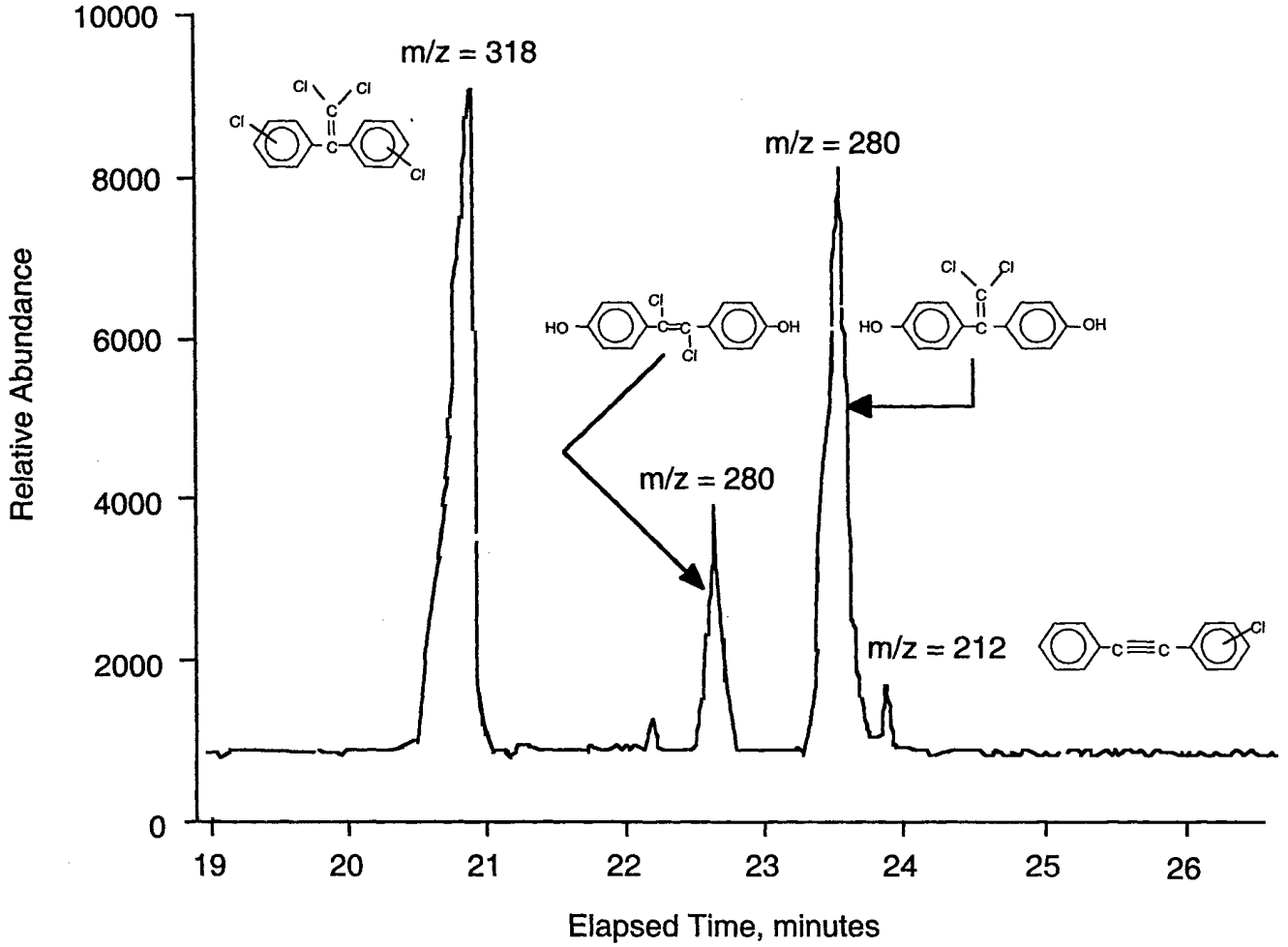

FIGURE E-4. GC MS OF BPC POLYCARBONATE CROSSLINKED

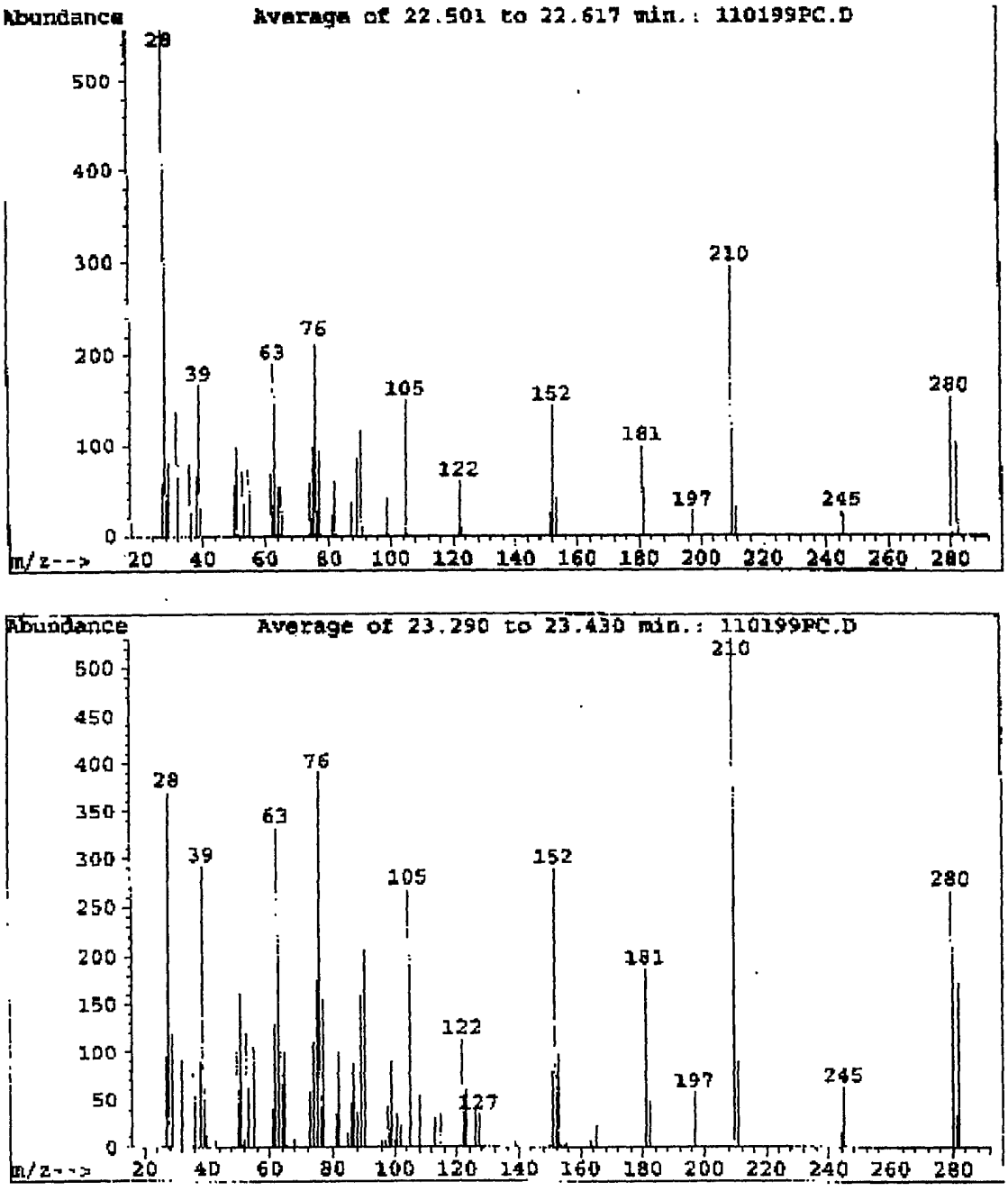

FIGURE E-5. COMPARISON OF THE MASS SPECTRA OF THE TWO SPECIES ASSUMED TO BE THE STILBENE (UP) AND THE 1,1-DICHLORO-2,2 BISPHENYL ETHYLENE (DOWN)